



**HAL**  
open science

## **A Specific Pattern of Phosphodiesterases Controls the cAMP Signals Generated by Different Gs-Coupled Receptors in Adult Rat Ventricular Myocytes.**

Francesca Rochais, Aniella Abi-Gerges, Kathleen Horner, Florence Lefebvre, Dermot M. F. Cooper, Marco Conti, Rodolphe Fischmeister, Grégoire Vandecasteele

### ► To cite this version:

Francesca Rochais, Aniella Abi-Gerges, Kathleen Horner, Florence Lefebvre, Dermot M. F. Cooper, et al.. A Specific Pattern of Phosphodiesterases Controls the cAMP Signals Generated by Different Gs-Coupled Receptors in Adult Rat Ventricular Myocytes.: PDEs and hormone specific cAMP signals. *Circulation Research*, 2006, 98 (8), pp.1081-8. 10.1161/01.RES.0000218493.09370.8e . inserm-00000047

**HAL Id: inserm-00000047**

**<https://www.hal.inserm.fr/inserm-00000047>**

Submitted on 7 Nov 2006

**HAL** is a multi-disciplinary open access archive for the deposit and dissemination of scientific research documents, whether they are published or not. The documents may come from teaching and research institutions in France or abroad, or from public or private research centers.

L'archive ouverte pluridisciplinaire **HAL**, est destinée au dépôt et à la diffusion de documents scientifiques de niveau recherche, publiés ou non, émanant des établissements d'enseignement et de recherche français ou étrangers, des laboratoires publics ou privés.

**Circulation Research Manuscript #CIRCRESAHA/2006/124800 - R1 Original Contribution**

This is an un-copyrighted author manuscript that was accepted for publication in *Circulation Research*, copyright The American Heart Association. This may not be duplicated or reproduced, other than for personal use or within the "Fair Use of Copyrighted Materials" (section 107, title 17, U.S. Code) without prior permission of the copyright owner, The American Heart Association. The final copyrighted article, which is the version of record, can be found at <http://circres.ahajournals.org/>. The American Heart Association disclaims any responsibility or liability for errors or omissions in this version of the manuscript or in any version derived from it.

**A Specific Pattern of Phosphodiesterases Controls the cAMP Signals Generated by Different G<sub>s</sub>-Coupled Receptors in Adult Rat Ventricular Myocytes****Francesca Rochais, Aniella Abi-Gerges, Kathleen Horner, Florence Lefebvre, Dermot M. F Cooper, Marco Conti, Rodolphe Fischmeister and Grégoire Vandecasteele**

From INSERM U-769 (F.R.,A.A.-G.,F.L., R.F., G.V.), Châtenay-Malabry, F-92296 France; Université Paris-Sud (F.R.,A.A.-G.,F.L., R.F., G.V.), Faculté de Pharmacie, Châtenay-Malabry, F-92296 France; Division of Reproductive Biology (K.H., M.C.), Department of Gynecology and Obstetrics, Stanford University, Stanford, USA; Department of Pharmacology (D.M.F.C.), University of Cambridge, Cambridge, UK.

running title : PDEs and hormone specific cAMP signals

*Correspondence to:*

Dr. Rodolphe FISCHMEISTER  
INSERM U-769  
Université de Paris-Sud  
Faculté de Pharmacie  
5, Rue J.-B. Clément  
F-92296 Châtenay-Malabry Cedex  
France

Tel. 33 1 46 83 57 57

Fax 33 1 46 83 54 75

E-mail: [fisch@vjf.inserm.fr](mailto:fisch@vjf.inserm.fr)

Subject codes: [152] Ion channels/membrane transport, [138] Cell signalling/signal transduction, [85] Autonomic, reflex, and neurohumoral control of circulation

**Abstract**—Compartmentation of cAMP is thought to generate the specificity of G<sub>s</sub>-coupled receptors action in cardiac myocytes, with phosphodiesterases (PDEs) playing a major role in this process by preventing cAMP diffusion. We have tested this hypothesis in adult rat ventricular myocytes (ARVMs) by characterizing PDEs involved in the regulation of cAMP signals and L-type Ca<sup>2+</sup> current ( $I_{Ca,L}$ ) upon stimulation with  $\beta_1$ -adrenergic receptors ( $\beta_1$ -AR),  $\beta_2$ -adrenergic receptors ( $\beta_2$ -AR), glucagon receptors (Glu-R) and prostaglandin E<sub>1</sub> receptors (PGE<sub>1</sub>-R). All receptors but PGE<sub>1</sub>-R increased total cAMP, and inhibition of PDEs with IBMX strongly potentiated these responses. When monitored in single cells by high affinity cyclic nucleotide-gated (CNG) channels, stimulation of  $\beta_1$ -AR and Glu-R increased cAMP, whereas  $\beta_2$ -AR and PGE<sub>1</sub>-R had no detectable effect. Selective inhibition of PDE3 by cilostamide and PDE4 by Ro 20-1724 potentiated  $\beta_1$ -AR cAMP signals, whereas Glu-R cAMP was augmented only by PD4 inhibition. PGE<sub>1</sub>-R and  $\beta_2$ -AR generated substantial cAMP increases only when PDE3 and PDE4 were blocked. For all receptors except PGE<sub>1</sub>-R, the measurements of  $I_{Ca,L}$  closely matched the ones obtained with CNG channels. Indeed, PDE3 and PDE4 controlled  $\beta_1$ -AR and  $\beta_2$ -AR regulation of  $I_{Ca,L}$ , while only PDE4 controlled Glu-R regulation of  $I_{Ca,L}$  thus demonstrating that receptor-PDE coupling has functional implications downstream of cAMP. PGE<sub>1</sub> had no effect on  $I_{Ca,L}$  even after blockade of PDE3 or PDE4, suggesting that other mechanisms prevent cAMP produced by PGE<sub>1</sub> to diffuse to L-type Ca<sup>2+</sup> channels. These results identify specific functional coupling of individual PDE families to G<sub>s</sub>-coupled receptors as a major mechanism enabling cardiac cells to generate heterogeneous cAMP signals in response to different hormones.

**Key words:** cAMP ■ heart ■ G protein-coupled receptor ■ phosphodiesterase

---

## Introduction

Cardiac myocytes express a number of G<sub>s</sub>-coupled receptors (G<sub>s</sub>PCRs) that raise intracellular cAMP levels and activate cAMP-dependent protein kinase (PKA) but exert different downstream effects. For instance, β<sub>1</sub>-AR stimulation produces a major and sustained increase in force of contraction, accelerates relaxation, and stimulates glycogen phosphorylase.<sup>1</sup> β<sub>2</sub>-AR stimulation also increases contractile force but does not activate glycogen phosphorylase<sup>2</sup> and does not accelerate relaxation<sup>1,3</sup> (but see Bartel *et al.* (2003)<sup>2</sup>); Glu-R stimulation activates phosphorylase and exerts positive inotropic and lusitropic effects, but the contractile effects fade with time.<sup>4</sup> Finally, PGE-1 has no effect on contractile activity or glycogen metabolism.<sup>5,6</sup>

Such observations led to the proposal that activation of different G<sub>s</sub>PCRs results in the accumulation of cAMP and phosphorylation of hormone target proteins in distinct compartments.<sup>7</sup> The discovery of A-kinase anchoring proteins, responsible for the subcellular distribution of particulate PKA,<sup>8</sup> and the development of new methodologies allowing to track local cAMP in living cells have provided additional support for this concept.<sup>9-15</sup>

Because cAMP is a small and readily diffusible molecule, cAMP compartments can only exist under a restrictive set of conditions for the localization and activity of the different components of the cAMP signaling cascade, namely G<sub>s</sub>PCRs, adenylyl cyclases, PKA and the cAMP phosphodiesterases (PDEs). Cardiac PDEs fall into four families: PDE1, which is activated by Ca<sup>2+</sup>/calmodulin; PDE2, which is stimulated by cGMP; PDE3, which is inhibited by cGMP; and PDE4. While PDE1 and PDE2 can hydrolyze both cAMP and cGMP, PDE3 preferentially hydrolyzes cAMP and PDE4 is specific for cAMP. Until now, only a limited number of studies have addressed directly the participation of PDEs to cAMP compartmentation and hormonal specificity in cardiac cells.<sup>9,10,12,15,16</sup> In a recent study, we used recombinant cyclic nucleotide-gated (CNG) channels as cAMP biosensors in adult rat

ventricular myocytes (ARVMs) to show that  $\beta$ -adrenergic cAMP signals are localized by PKA-mediated activation of PDE3 and/or PDE4.<sup>13</sup> However, PDE regulation of other hormonal cAMP signals is presently unknown. In the following, we address this point by comparing the cAMP signals generated by  $\beta_1$ -AR,  $\beta_2$ -AR, Glu-R and PGE<sub>1</sub>-R, their regulation by individual PDE families, and the functional consequences on L-type Ca<sup>2+</sup> channels.

## Materials and Methods

Detailed methods are included in the online-only Data Supplement to this article, which is available at <http://www.circres.ahajournals.org>.

*Total cAMP determination* - cAMP was measured by RIA after acetylation of the samples.<sup>20,21</sup>

*PDE Assay*- PDE activity was measured according to a modification of the two-step assay procedure method described by Thompson & Appleman<sup>17</sup> with 1  $\mu$ M cAMP and  $10^5$  cpm [<sup>3</sup>H]-cAMP, as detailed previously.<sup>18</sup>

*Electrophysiological Experiments* - The whole-cell configuration of the patch-clamp technique was used to record the L-type calcium current ( $I_{Ca,L}$ ) and the CNG current ( $I_{CNG}$ ). The extracellular Cs<sup>+</sup>-Ringer solution contained 1.8 mM [Ca<sup>2+</sup>] and 1.8 mM [Mg<sup>2+</sup>] for  $I_{Ca,L}$  recordings and nominal [Ca<sup>2+</sup>] and [Mg<sup>2+</sup>] plus 1  $\mu$ mol/L nifedipine for  $I_{CNG}$  recordings. Patch pipettes were filled with a Cs<sup>+</sup>-solution.

*Data Analysis* -  $I_{Ca,L}$  amplitude was measured as the difference between the peak inward current and the current at the end of the 400-ms duration pulse.<sup>19</sup>  $I_{CNG}$  amplitude was measured at the end of the 200 ms pulse. Capacitance and leak currents were not compensated. In 141 ARVMs, mean capacitance was  $160.5 \pm 3.9$  pF.  $I_{CNG}$  density was calculated for each experiment as the ratio of current amplitude to cell capacitance. All the data are expressed as mean  $\pm$  S.E.M. When appropriate, the Student's *t*-test was used for statistical evaluation.

## Results

### PDE activities in ARVMs

Figure 1 summarizes experiments where the relative activity of PDE2, PDE3 and PDE4 in quiescent ARVMs was determined. Total cAMP hydrolytic activity was on average  $109.8 \pm 16.6$  pmoles/min/mg protein ( $n=4$ ) and was mainly due to PDE3 and PDE4, which represented 31% and 38% of the total, respectively. Under these assay conditions, PDE2 activity was minimal (Fig. 1). Immunoprecipitation experiments showed that PDE4 activity is contributed by PDE4A, PDE4B and PDE4D variants, while the PDE3A form is the predominant PDE3 expressed (data not shown). The relative activity of individual PDE families did not vary significantly after 24 h and 48 h of culture (data not shown). Moreover, the ratio of PDE3/PDE4 was similar to that measured in extracts of adult rat ventricle (data not shown). Thus, cultured ARVMs closely resemble the *in vivo* pattern of PDE expression.

(Figure 1 near here)

### Total cAMP production in response to different GsPCRs in ARVMs

We next determined whether stimulation of different GsPCRs increased total cAMP in ARVMs (Fig. 2). We used a combination of isoprenaline (ISO, 5  $\mu\text{mol/L}$ ) and the  $\beta_2$ -AR antagonist ICI 118551 (ICI, 1  $\mu\text{mol/L}$ ) to stimulate  $\beta_1$ -AR, a combination of ISO (5  $\mu\text{mol/L}$ ) in the presence of the  $\beta_1$ -AR antagonist CGP 20712A (CGP, 1  $\mu\text{mol/L}$ ) to stimulate the  $\beta_2$ -AR, glucagon (Glu, 1  $\mu\text{mol/L}$ ) to stimulate Glu-R, and PGE<sub>1</sub> (1  $\mu\text{mol/L}$ ) to stimulate PGE<sub>1</sub>-R. Basal cAMP was more than doubled by ISO + ICI and Glu, and increased by  $\approx 70\%$  by ISO + CGP. PGE<sub>1</sub> had no effect on cAMP content under these experimental conditions. A 15 min incubation with the broad spectrum PDE inhibitor IBMX (100  $\mu\text{mol/L}$ ) increased the total cAMP content by about two-fold and dramatically potentiated the response to all agonists

except PGE<sub>1</sub>. The effect of ISO + ICI and Glu were multiplied by 8 and 7, respectively, while that of ISO + CGP was increased 3-fold. Cyclic AMP content after PGE<sub>1</sub> + IBMX was slightly increased when compared to IBMX alone although it did not reach statistical significance.

(Figure 2 near here)

### **Real-time monitoring of subsarcolemmal cAMP signals elicited by different GsPCRs in ARVMs**

To further compare cAMP signals elicited by the different receptors, we used CNG channels that allow direct monitoring of cAMP variations beneath the plasma membrane in intact ARVMs.<sup>13</sup> Figure 3 summarizes the results obtained with two CNGA2 mutants which differ in their sensitivity to cAMP, E583M (EC<sub>50</sub> for cAMP ≈10 μmol/L) and C460W/E583M (EC<sub>50</sub> for cAMP ≈1 μmol/L).<sup>20</sup> As depicted in Fig. 3A, activation of β<sub>1</sub>-AR by a combination of ISO (5 μmol/L) and ICI (1 μmol/L) increased basal *I*<sub>CNG</sub> density ≈3-fold, whereas specific activation of β<sub>2</sub>-AR by ISO (5 μmol/L) plus CGP (1 μmol/L) had no effect. Similarly, activation of Glu-R by Glu (1 μmol/L) or PGE<sub>1</sub>-R by PGE<sub>1</sub> (1 μmol/L) failed to activate *I*<sub>CNG</sub> (Fig. 3A). These results indicate that cAMP concentration was below the activation threshold of E583M CNGA2 upon stimulation of β<sub>2</sub>-AR, Glu-R and PGE<sub>1</sub>-R. When using the C460W/E583M mutant (Fig. 3B), activation of β<sub>1</sub>-AR increased basal *I*<sub>CNG</sub> density 6-fold. This effect was significantly higher (p<0.01) than that obtained in cells expressing E583M CNGA2, as expected from the relative affinities of the two channels toward cAMP. Interestingly, application of Glu now activated *I*<sub>CNG</sub> by approximately 5-fold, but specific activation of β<sub>2</sub>-AR or PGE<sub>1</sub>-R still had no effect. Thus, the increased sensitivity of



C460W/E583M CNGA2 allowed the detection of subsarcolemmal cAMP generated by activation of Glu-R but not by activation of  $\beta_2$ -AR or PGE<sub>1</sub>-R.

(Figure 3 near here)

### **Regulation of subsarcolemmal cAMP signals by PDEs**

The above results suggest that cAMP signals elicited by the four different G<sub>s</sub>PCRs at the plasma membrane are not identical. We next investigated the contribution of PDEs to such specificity. Both CNGA2 mutants were used with essentially similar results, therefore the low affinity E583M channel data are presented as supplementary Figures I and II. Preliminary experiments showed that IBMX (100  $\mu$ mol/L) had no significant effect on  $I_{\text{CNG}}$  from myocytes expressing E583M/C460W (n=6, data not shown). Figure 4A shows a typical experiment in which the amplitude of  $I_{\text{CNG}}$  is depicted as a function of time, thus providing an instant readout of subsarcolemmal cAMP level in a single cardiac myocyte.  $\beta_1$ -AR stimulation with ISO (5  $\mu$ mol/L) + ICI (1  $\mu$ mol/L) induced a substantial increase of  $I_{\text{CNG}}$ , which was strongly potentiated by selective PDE3 inhibition with cilostamide (Cil, 1  $\mu$ mol/L) or selective PDE4 inhibition with Ro 20-1724 (Ro, 10  $\mu$ mol/L). Concomitant inhibition of all PDEs with IBMX (100  $\mu$ mol/L) resulted in a similar potentiation of  $\beta_1$ -AR stimulation to that obtained with selective PDE4 inhibition. At the end of each experiment, the cell was challenged with a saturating concentration (100  $\mu$ mol/L) of the forskolin analog L-858051 (L-85) to determine the maximal  $I_{\text{CNG}}$  response. In Figures 4C and 4D, we investigated the role of PDEs in shaping the  $\beta_2$ -AR cAMP response. As seen before, application of ISO (5  $\mu$ mol/L) + CGP (1  $\mu$ mol/L) had no effect on  $I_{\text{CNG}}$ . Selective inhibition of PDE3 during  $\beta_2$ -AR stimulation with ISO + CGP induced a small and transient increase of  $I_{\text{CNG}}$ . A somewhat stronger effect was observed upon PDE4 inhibition, although it was also transient (Fig. 4C).

In contrast, concomitant inhibition of PDE3 and PDE4 unmasked a robust and sustained cAMP increase during  $\beta_2$ -AR stimulation. These results indicate that PDE3 and PDE4 control cAMP elicited by  $\beta_1$ -AR and  $\beta_2$ -AR. Both PDEs are necessary to circumvent the cAMP rise elicited by  $\beta_1$ -AR, while either PDE3 or PDE4 individually are sufficient to prevent cAMP to rise beneath membrane upon  $\beta_2$ -AR activation.

(Figure 4 near here)

Figure 5A shows that inhibition of PDE3 had little effect on  $I_{\text{CNG}}$  augmented by 1  $\mu\text{mol/L}$  Glu while a selective inhibition of PDE4 by Ro produced a strong stimulation of the current. Concomitant inhibition of both PDE3 and PDE4 by Cil + Ro, or of all PDEs by IBMX, resulted in a comparable effect as inhibition of PDE4 alone (Fig. 5A and 5B). These results indicate that Glu-R cAMP signals at the membrane are exclusively controlled by PDE4. Although no increase in cAMP with  $\text{PGE}_1$  could be detected before, we tested whether PDE inhibition could reveal a  $\text{PGE}_1$  effect on  $I_{\text{CNG}}$ . As shown in Fig. 5C, application of 1  $\mu\text{mol/L}$   $\text{PGE}_1$  did not affect  $I_{\text{CNG}}$ . However, in the continuous presence of  $\text{PGE}_1$ , simultaneous inhibition of PDE3 and PDE4 (by Cil + Ro) clearly activated the CNG current. IBMX was more efficient than Cil + Ro, indicating that other PDEs besides PDE3 and PDE4 might play a role under these conditions (Fig. 5C). Thus, similarly to  $\beta_2$ -AR, cAMP mobilization by  $\text{PGE}_1$ -R needs concomitant inhibition of PDE3 and PDE4 to be detected at the membrane. However, in contrast to  $\beta_2$ -AR, other PDEs besides PDE3 and PDE4 regulate  $\text{PGE}_1$ -R cAMP signals in cardiac cells.

(Figure 5 near here)

### Regulation of the L-type $\text{Ca}^{2+}$ current by GsPCRs and PDEs

Collectively, the above results show that different PDEs are involved in the regulation of cAMP generated by distinct GsPCRs in cardiac myocytes. In order to evaluate the functional implication of these findings, we examined the regulation of a major sarcolemmal cAMP target, the L-type  $\text{Ca}^{2+}$  current ( $I_{\text{Ca,L}}$ ), by GsPCRs and PDEs. The experiments were performed at 24 h, as with CNG channels experiments. Selective inhibition of PDE3 by Cil (1  $\mu\text{mol/L}$ ) or PDE4 by Ro (10  $\mu\text{mol/L}$ ) had no effect on basal  $I_{\text{Ca,L}}$  (data not shown). As the concentration of ISO (5  $\mu\text{mol/L}$ ) used in the  $\beta_1$ -AR stimulation of  $I_{\text{CNG}}$  produced a maximal stimulation of  $I_{\text{Ca,L}}$  (121.3 $\pm$ 22.2% over control, n=9, data not shown), a lower dose of ISO (1 nmol/L, with 1  $\mu\text{mol/L}$  ICI) was used in subsequent experiments in order to assess the contribution of PDE isoforms to the  $\beta_1$ -AR regulation of  $I_{\text{Ca,L}}$ . In these conditions, selective inhibition of PDE3 by Cil or PDE4 by Ro resulted in a marked potentiation of the prestimulated  $I_{\text{Ca,L}}$  (Fig. 6A and 6B). As shown in Fig. 6C and 6D,  $\beta_2$ -AR stimulation with ISO (5  $\mu\text{mol/L}$ ) and CGP (1  $\mu\text{mol/L}$ ) produced a small but significant stimulation of  $I_{\text{Ca,L}}$ . This effect could be further potentiated by PDE3 inhibition with Cil and more markedly by PDE4 blockade with Ro. These results indicate that PDE3, and more prominently PDE4, are integral components of  $I_{\text{Ca,L}}$  regulation by  $\beta_1$ -AR and  $\beta_2$ -AR. In another series of experiments, the regulation of  $I_{\text{Ca,L}}$  by Glu was investigated. At high (1  $\mu\text{mol/L}$ ) concentration, Glu maximally stimulated  $I_{\text{Ca,L}}$  and addition of PDE inhibitors had no effect (data not shown). At the concentration of 10 nmol/L, Glu slightly decreased  $I_{\text{Ca,L}}$  and PDE3 inhibition by Cil had no effect. However, application of Ro to block PDE4 clearly increased  $I_{\text{Ca,L}}$  (Fig. 7A and 7B). Finally, as shown in Fig. 7C and 7D,  $\text{PGE}_1$  had no effect on  $I_{\text{Ca,L}}$ , even when either PDE3 or PDE4 was blocked. However, concomitant inhibition of PDE3 and PDE4 increased  $I_{\text{Ca,L}}$  in the presence of  $\text{PGE}_1$ , but this effect was not different from the effect of the inhibitors on the basal  $I_{\text{Ca,L}}$  (Fig. 7D). These results confirm the specific and functional coupling of Glu-R to

PDE4, and show that the cAMP compartment generated by activation of PGE<sub>1</sub>-R is not in contact with L-type Ca<sup>2+</sup> channels.

(Figure 6 and 7 near here)

## Discussion

While a number of recent studies have underscored the role of PDEs in tailoring hormonal cAMP signals,<sup>9-13,21-23</sup> none has addressed directly whether distinct hormonal cAMP signals are controlled by different PDEs. To gain some insight into this question, we used complementary biochemical and electrophysiological techniques to resolve cAMP at the cellular, subsarcolemmal and local levels. We show that four canonical G<sub>s</sub>PCRs expressed in ARVMs generate different cAMP signals due to a specific contribution of individual PDE families. For all receptors but PGE<sub>1</sub>-R, the nature of this functional coupling determines the regulation of a major downstream cAMP target, the L-type Ca<sup>2+</sup> channels.

In agreement with previous studies, we found that PDE3 and PDE4 represent the major cAMP hydrolytic activities in rodent cardiomyocytes.<sup>12,13,24</sup> While there is a general agreement that  $\beta_1$ -AR increases cAMP in adult rat cardiac preparations,<sup>3,25-27</sup> the ability of  $\beta_2$ -AR to do so is a matter of debate.<sup>3,25,26</sup> Although glucagon increases cAMP in various cardiac preparations,<sup>4</sup> recent studies failed to detect it.<sup>27,28</sup> Thus, we checked whether stimulation of the different receptors led to detectable increases in total cAMP in ARVMs. We found that stimulation of  $\beta_1$ -AR, Glu-R, and to a lesser extent  $\beta_2$ -AR, increased total cAMP content, and that IBMX greatly accentuated these effects. In contrast, PGE<sub>1</sub> alone did not increase cAMP, although a small effect could be observed in the presence of IBMX. This result is at variance with those from Buxton & Brunton<sup>29</sup> in rabbit cardiomyocytes, where ISO and PGE<sub>1</sub> similarly increased cAMP. However, in addition to species differences, the experimental conditions used here are different, as PGE<sub>1</sub> was used at a 10-fold lower concentration (1 vs. 10  $\mu$ mol/L) and application lasted 5-fold less (3 vs. 15 min).

We next used CNG channels to monitor cAMP signals triggered by distinct routes near the plasma membrane.<sup>11,13</sup> We found that activation of  $\beta_1$ -AR and Glu-R elicit readily

detectable cAMP at the membrane, whereas  $\beta_2$ -AR and PGE<sub>1</sub>-R do not. In heterologous expression systems and in rat olfactory epithelium, CNG channels associate preferentially with non-caveolar lipid rafts.<sup>30</sup> If this holds true in ARVMs, failure to detect cAMP elicited by  $\beta_2$ -AR and PGE<sub>1</sub>-R could be due to localization of these receptors in caveolae.<sup>31-34</sup> However, this localization does not prevent cAMP diffusion to CNG channels when PDEs are inhibited. Indeed, we found that IBMX, at 100  $\mu$ mol/L concentration, increased the response of  $I_{\text{CNG}}$  not only to  $\beta_1$ -AR and Glu-R stimulation, but also revealed cAMP generated by  $\beta_2$ -AR and PGE<sub>1</sub>-R stimulation. Given the  $K_i$  of IBMX for the different PDEs,<sup>35</sup> 100  $\mu$ mol/L of this inhibitor should block most of the PDE activity, PDE1, PDE2, PDE3 and PDE4 being inhibited by  $\approx 98\%$ ,  $\approx 93\%$ ,  $\approx 97\%$  and  $\approx 87\%$ , respectively. To delineate the specific contribution of PDE4, we used Ro 20-1724, which at 10  $\mu$ mol/L should inhibit  $\approx 71\%$  of its activity without affecting the other PDEs.<sup>35</sup> We found that PDE4 hydrolyzes cAMP produced by all the receptors tested, thus limiting PKA activation and  $\text{Ca}^{2+}$  channel phosphorylation upon  $\beta_1$ -AR,  $\beta_2$ -AR and Glu-R activation. These results are consistent with previous studies showing that PDE4 is critically involved in the regulation of  $I_{\text{Ca,L}}$  and contractility by catecholamines and glucagon.<sup>21,28,36</sup> PDE4 isoforms are likely to play this ubiquitous role due to their molecular diversity and specific subcellular localization.<sup>37-39</sup> However, whether specific PDE4 isoforms are associated with different receptors remains unclear. Recent data in neonatal cardiomyocytes reported an important role for PDE4B2 in controlling norepinephrine-induced cAMP increase.<sup>12</sup> However, in the same model, other studies suggest that PDE4D isoforms are preferentially associated with the  $\beta_2$ -AR. For instance, PDE4D5 and to a lesser extent PDE4D3 are recruited to the  $\beta_2$ -AR by  $\beta$ -arrestin upon ISO challenge.<sup>22,40</sup> Moreover, Xiang et al. (2005)<sup>16</sup> showed that PDE4D selectively affects  $\beta_2$ -AR vs.  $\beta_1$ -AR positive chronotropism. Whether these findings apply to ARVMs remains to be established.

Nearly complete ( $\approx 95\%$ ) and selective PDE3 inhibition should be achieved by 1  $\mu\text{mol/L}$  cilostamide<sup>35</sup>. Using this inhibitor, we found that PDE3 controls the cAMP signals generated by  $\beta_1$ -AR,  $\beta_2$ -AR and PGE<sub>1</sub>-R, but not Glu-R. However, on  $I_{\text{Ca,L}}$  response, PDE3 controlled the effects of  $\beta_1$ -AR and  $\beta_2$ -AR, but had no impact on Glu-R or PGE<sub>1</sub>-R stimulation. We showed previously that PDE3 controlled cAMP diffusion and consequently  $I_{\text{Ca,L}}$  activation in cardiac myocytes subjected to  $\beta$ -adrenergic stimulation.<sup>13,21,36,41,42</sup> Our findings contrast with results obtained in neonatal rat ventricular myocytes where PDE3 was found to have a moderate effect on  $\beta_1$ -AR (with norepinephrine) induced cAMP.<sup>12</sup> Moreover, in right ventricular strips from adult rat, PDE3 inhibition had no effect on the contractile response to the  $\beta_1$ -AR agonist dobutamine but potentiated that of glucagon.<sup>27</sup> In parallel cAMP assays, these authors found that PDE3 inhibition had also no effect on the response to dobutamine but revealed a substantial cAMP increase caused by glucagon. While obvious differences in developmental stage, cardiac territory or rat strains might account for some of the discrepancies, one should emphasize that CNG channels provide a readout of subsarcolemmal cAMP, while other methods measure cytosolic or total cAMP. Thus, one could speculate that upon  $\beta_1$ -AR stimulation, PDE3 controls the membrane cAMP pool but not a cytosolic one, possibly involved in contractility (sarcoplasmic reticulum-associated PDE3 for instance<sup>43</sup>). In the case of Glu-R, the opposite would be true: PDE3 would not control subsarcolemmal cAMP generated by Glu-R, but would prevent the access of the second messenger to other, non sarcolemmal inotropic targets. For such a hypothesis to be valid, one must further speculate either that totally segregated cAMP pathways are triggered by the different receptors (including PKA targets), or that differential regulation of PDE3 is triggered by receptor activation. The latter mechanisms was found in frog heart but not in rat.<sup>44</sup>

While inhibition of either PDE3 or PDE4 potentiated the  $\beta_1$ -AR response, and selective inhibition of PDE4 only potentiated the response to Glu, concomitant inhibition of both low  $K_m$  cAMP PDEs was necessary to observe a substantial cAMP accumulation upon  $\beta_2$ -AR and PGE<sub>1</sub>-R stimulations. This indicates that both PDE3 and PDE4 are functionally associated with  $\beta_2$ -AR and PGE<sub>1</sub>-R, but that one is sufficient to lower cAMP below the detection threshold of CNG channels. When examining the regulation of  $I_{Ca,L}$  by  $\beta_2$ -AR, single inhibition of PDE3 or PDE4 potentiated the effect of ISO+CGP. This may reflect the  $\approx$ 3-10-fold higher sensitivity of PKA vs. CNG channels to cAMP. In contrast, single inhibition of PDE3 or PDE4 failed to reveal any effect of PGE<sub>1</sub> on  $I_{Ca,L}$ . Although concomitant inhibition of both PDEs readily stimulate  $I_{Ca,L}$  in these cells and may mask a PGE<sub>1</sub> effect (Fig. 7D), the data suggest that PGE<sub>1</sub>-R lie in a distinct compartment from L-type Ca<sup>2+</sup> channels.

Upon stimulation of  $\beta_1$ -AR,  $\beta_2$ -AR, and Glu-R, inhibition of PDE1-4 by IBMX had a similar effect on  $I_{CNG}$  as did concomitant PDE3 and PDE4 inhibition. This suggests that no other PDE, besides PDE3 and PDE4, played a significant role under our experimental conditions. However, a very different situation occurred with PGE<sub>1</sub>: in this case, inhibition of PDE1-4 by IBMX had a greater effect than concomitant inhibition of PDE3 and PDE4. Thus, other PDEs, most likely PDE1 or PDE2, may also regulate PGE<sub>1</sub>-R-mediated intracellular cAMP signals.

Although this study was performed on healthy cardiac myocytes, it is tempting to speculate that changes in the organization of the cAMP compartments might take place in pathological conditions, such as heart failure. Cardiac hypertrophy and failure are associated with a profound remodeling of the cAMP signaling pathway in cardiomyocytes<sup>45</sup> As to changes in PDE expression or activity, the results published so far are limited and contradictory. In rapid pacing-induced heart failure in dog, PDE3 mRNA and activity were



decreased while PDE4D was unchanged.<sup>46</sup> In the same model, a modest reduction in total PDE activity was found in the left ventricular subendocardium but not in the epicardium, suggesting regional differences.<sup>47</sup> In human, sarcoplasmic reticulum-associated PDE3 activity was shown to be unchanged in heart failure,<sup>43</sup> although total PDE3 activity appears reduced and PDE3A protein expression down-regulated in end-stage failing human heart.<sup>48</sup> In rat, the expression and activity of PDE3 and PDE4 are strongly augmented in hypertension-induced hypertrophy.<sup>49</sup> Finally, a recent study shows that PDE4D deficiency favours ryanodine receptors aberrant phosphorylation and promotes heart failure in mice.<sup>50</sup> Although more work is needed to obtain a clear picture of the PDE rearrangement occurring in hypertrophy and heart failure, this study suggests that PDE alteration may affect cAMP compartmentation, leading to untargeted hormonal cAMP signals, aberrant phosphorylation of targets proteins and, *in fine*, contribute to cardiac dysfunction.

## **Acknowledgements**

We thank Patrick Lechêne (INSERM U769) for skilful technical assistance and Dr. Frank Lezoualc'h for critical reading of the manuscript. This work was supported by an INSERM fellowship (to M.C.), Fondation de France (to G.V.), French Ministry of Education and Research (F.R. and A.A.-G.), Association Française contre les Myopathies (F.R.), National Institutes of Health (RO1 HD 20788) (to M.C. and K.H.) and by European Union Contract n°LSHM-CT-2005-018833/EUGeneHeart (to R.F.).

## **Conflict of interest statement**

None.

## Figure legends

**Figure 1.** Relative PDE activities in ARVMs. PDE2 activity was determined as the fraction of total hydrolytic activity inhibited by 10  $\mu\text{mol/L}$  EHNA; PDE3 as the fraction inhibited by 1  $\mu\text{mol/L}$  cilostamide; and PDE4 activity as the fraction inhibited by 1  $\mu\text{mol/L}$  rolipram. To some instances, rolipram was replaced by RS25344 (1  $\mu\text{mol/L}$ ) or piclamilast (1  $\mu\text{mol/L}$ ) with identical results. The bars represent the mean $\pm$ s.e.m of the number of independent experiments indicated.

**Figure 2.** Effect of various stimuli linked to adenylyl cyclase activation on total cAMP content in freshly isolated ARVMs. Where necessary, the  $\beta_1$ -AR antagonist CGP 20712A (CGP, 1  $\mu\text{mol/L}$ ), the  $\beta_2$ -AR antagonist ICI 118551 (ICI, 1  $\mu\text{mol/L}$ ) and IBMX (100  $\mu\text{mol/L}$ ) were added 15 min before the 3 min stimulation with ISO (5  $\mu\text{mol/L}$ ), glucagon (Glu, 1  $\mu\text{mol/L}$ ) or PGE<sub>1</sub> (1  $\mu\text{mol/L}$ ). The bars show the means $\pm$ s.e.m. of the number of experiments indicated near the bars. Statistically significant difference in cAMP content between basal and agonists alones or between IBMX and agonists with IBMX are indicated as \*\*\*,  $p < 0.001$ .

**Figure 3.** Subsarcolemmal cAMP signals reported by CNG channels upon activation of distinct GsPCRs in ARVMs. CNG current ( $I_{\text{CNG}}$ ) density from recombinant E583M (A) and C460W/E583M (B) CNGA2 channels was measured by the whole-cell patch-clamp technique in rat ventricular myocytes 24 h after isolation. Activation of  $\beta_1$ -AR was achieved by application of isoprenaline (ISO, 5  $\mu\text{mol/L}$ ) in the presence of the ICI 118551 (ICI, 1  $\mu\text{mol/L}$ ). Activation of  $\beta_2$ -AR was done by application of ISO (5  $\mu\text{mol/L}$ ) in combination with CGP 20712A (CGP, 1  $\mu\text{mol/L}$ ). Activation of Glu-R (C) and PGE<sub>1</sub>-R (D) was done by application of glucagon (Glu, 1  $\mu\text{mol/L}$ ) and PGE<sub>1</sub> (1  $\mu\text{mol/L}$ ). Statistically significant differences are indicated as \*,  $p < 0.05$  ; \*\*,  $p < 0.01$  and \*\*\*,  $p < 0.001$ .

**Figure 4.** PDE regulation of cAMP signals from  $\beta_1$ -AR and  $\beta_2$ -AR. A and C, Time course of  $I_{\text{CNG}}$  in ARVMs expressing C460W/E583M CNGA2. The cells were first superfused with control external Ringer and then challenged with the drugs during the periods indicated by the solid lines. B and D, Summary of the results obtained in a series of experiments as in A and C, respectively. Specific activation of  $\beta_1$ -AR and  $\beta_2$ -AR as in Fig. 1. Selective PDE3 inhibition by cilostamide (Cil, 1  $\mu\text{mol/L}$ ) or selective PDE4 inhibition by Ro 20-1724 (Ro, 10  $\mu\text{mol/L}$ ) strongly potentiated cAMP triggered by  $\beta_1$ -AR. Upon activation of  $\beta_2$ -AR, robust cAMP accumulation necessitated concomitant PDE3 and PDE4 blockade. Experiment was ended with application of 100  $\mu\text{mol/L}$  L-85. .Statistically significant differences as in figure 3.

**Figure 5.** PDE regulation of cAMP signals from Glu-R and  $\text{PGE}_1$ -R. A and C, Time course of  $I_{\text{CNG}}$  in ARVMs expressing C460W/E583M CNGA2. B and D, Summary of the results obtained in a series of experiments as in A and C, respectively. A and B, Cil (1  $\mu\text{mol/L}$ ) exerted a transient potentiation of  $I_{\text{CNG}}$  previously enhanced by glucagon (Glu, 1  $\mu\text{mol/L}$ ), while Ro (10  $\mu\text{mol/L}$ ) exerted a major and sustained cAMP accumulation. C and D, The cAMP response to  $\text{PGE}_1$  was revealed at the membrane by simultaneous blockade of PDE3 and PDE4 and further increased by application of IBMX. Statistically significant differences are indicated as \*,  $p < 0.05$ .

**Figure 6.** Regulation of  $I_{\text{Ca,L}}$  by  $\beta$ -AR and PDEs. A and C, Time course of  $I_{\text{Ca,L}}$  in ARVMs cultured for 24h. The cells were first superfused with control external Ringer and then challenged with the drugs during the periods indicated by the solid lines. ISO was used at 1 nmol/L in A and B, and at 5  $\mu\text{mol/L}$  in C and D; all other drugs as in previous figures. B and

D, Summary of the results obtained in a series of experiments as in A and C, respectively. Statistically significant differences indicated as in previous figures.

**Figure 7.** Regulation of  $I_{Ca,L}$  by Glu-R, PGE<sub>1</sub>-R and PDEs. A and C, Time course of  $I_{Ca,L}$  in ARVMs cultured for 24h. Glucagon (Glu) was used at 1 nmol/L in A and B; all other drugs as in previous figures. B and D, Summary of the results obtained in a series of experiments as in A and C, respectively. Statistically significant differences indicated as in previous figures. NS, non significant.

## References

1. Xiao RP, Lakatta EG. Beta 1-adrenoceptor stimulation and beta 2-adrenoceptor stimulation differ in their effects on contraction, cytosolic Ca<sup>2+</sup>, and Ca<sup>2+</sup> current in single rat ventricular cells. *Circ Res.* 1993;73:286-300.
2. Bartel S, Krause EG, Wallukat G, Karczewski P. New insights into beta2-adrenoceptor signaling in the adult rat heart. *Cardiovasc Res.* 2003;57:694-703.
3. Kuznetsov V, Pak E, Robinson RB, Steinberg SF. Beta 2-adrenergic receptor actions in neonatal and adult rat ventricular myocytes. *Circ Res.* 1995;76:40-52.
4. Farah AE. Glucagon and the circulation. *Pharmacol Rev.* 1983;35:181-217.
5. Hayes JS, Brunton LL, Brown JH, Reese JB, Mayer SE. Hormonally specific expression of cardiac protein kinase activity. *Proc Natl Acad Sci U S A.* 1979;76:1570-1574.
6. Brunton LL, Hayes JS, Mayer SE. Hormonally specific phosphorylation of cardiac troponin I and activation of glycogen phosphorylase. *Nature.* 1979;280:78-80.
7. Steinberg SF, Brunton LL. Compartmentation of G protein-coupled signaling pathways in cardiac myocytes. *Annu Rev Pharmacol Toxicol.* 2001;41:751-773.
8. Wong W, Scott JD. AKAP signalling complexes: focal points in space and time. *Nat Rev Mol Cell Biol.* 2004;5:959-970.
9. Jurevicius J, Fischmeister R. cAMP compartmentation is responsible for a local activation of cardiac Ca<sup>2+</sup> channels by beta-adrenergic agonists. *Proc Natl Acad Sci U S A.* 1996;93:295-299.
10. Zaccolo M, Pozzan T. Discrete microdomains with high concentration of cAMP in

- stimulated rat neonatal cardiac myocytes. *Science*. 2002;295:1711-1715.
11. Rich TC, Fagan KA, Tse TE, Schaack J, Cooper DM, Karpen JW. A uniform extracellular stimulus triggers distinct cAMP signals in different compartments of a simple cell. *Proc Natl Acad Sci U S A*. 2001;98:13049-13054.
  12. Mongillo M, McSorley T, Evellin S, Sood A, Lissandron V, Terrin A, Huston E, Hannawacker A, Lohse MJ, Pozzan T, Houslay MD, Zaccolo M. Fluorescence resonance energy transfer-based analysis of cAMP dynamics in live neonatal rat cardiac myocytes reveals distinct functions of compartmentalized phosphodiesterases. *Circ Res*. 2004;95:67-75.
  13. Rochais F, Vandecasteele G, Lefebvre F, Lugnier C, Lum H, Mazet JL, Cooper DM, Fischmeister R. Negative feedback exerted by cAMP-dependent protein kinase and cAMP phosphodiesterase on subsarcolemmal cAMP signals in intact cardiac myocytes: an in vivo study using adenovirus-mediated expression of CNG channels. *J Biol Chem*. 2004;279:52095-52105.
  14. Warriar S, Belevych AE, Ruse M, Eckert RL, Zaccolo M, Pozzan T, Harvey RD. Beta-adrenergic- and muscarinic receptor-induced changes in cAMP activity in adult cardiac myocytes detected with FRET-based biosensor. *Am J Physiol Cell Physiol*. 2005;289:C455-461.
  15. Mongillo M, Tocchetti CG, Terrin A, Lissandron V, Cheung YF, Dostmann WR, Pozzan T, Kass DA, Paolocci N, Houslay MD, Zaccolo M. Compartmentalized Phosphodiesterase-2 Activity Blunts  $\beta$ -Adrenergic Cardiac Inotropy via an NO/cGMP-Dependent Pathway. *Circ Res*. 2006;98:226-234.
  16. Xiang Y, Naro F, Zoudilova M, Jin SL, Conti M, Kobilka B. Phosphodiesterase 4D is

- required for  $\beta_2$  adrenoceptor subtype-specific signaling in cardiac myocytes. *Proc Natl Acad Sci U S A*. 2005;102:909-914.
17. Thompson WJ, Appleman MM. Multiple cyclic nucleotide phosphodiesterase activities from rat brain. *Biochemistry*. 1971;10:311-316.
  18. Oki N, Takahashi SI, Hidaka H, Conti M. Short term feedback regulation of cAMP in FRTL-5 thyroid cells. Role of PDE4D3 phosphodiesterase activation. *J Biol Chem*. 2000;275:10831-10837.
  19. Kirstein M, Rivet-Bastide M, Hatem S, Benardeau A, Mercadier JJ, Fischmeister R. Nitric oxide regulates the calcium current in isolated human atrial myocytes. *J Clin Invest* 1995;95:794-802.
  20. Rich TC, Tse TE, Rohan JG, Schaack J, Karpen JW. In vivo assessment of local phosphodiesterase activity using tailored cyclic nucleotide-gated channels as cAMP sensors. *J Gen Physiol*. 2001;118:63-78.
  21. Jurevicius J, Skeberdis VA, Fischmeister R. Role of cyclic nucleotide phosphodiesterase isoforms in cAMP compartmentation following beta2-adrenergic stimulation of ICa,L in frog ventricular myocytes. *J Physiol*. 2003;551:239-252.
  22. Baillie GS, Sood A, McPhee I, Gall I, Perry SJ, Lefkowitz RJ, Houslay MD. beta-Arrestin-mediated PDE4 cAMP phosphodiesterase recruitment regulates beta-adrenoceptor switching from Gs to Gi. *Proc Natl Acad Sci U S A*. 2003;100:940-945.
  23. Barnes AP, Livera G, Huang P, Sun C, O'neal WK, Conti M, Stutts MJ, Milgram SL. Phosphodiesterase 4D Forms a cAMP diffusion barrier at the apical membrane of the airway epithelium. *J Biol Chem*. 2004;280:7997-8003.

24. Georget M, Mateo P, Vandecasteele G, Lipskaia L, Defer N, Hanoune J, Hoerter J, Lugnier C, Fischmeister R. Cyclic AMP compartmentation due to increased cAMP-phosphodiesterase activity in transgenic mice with a cardiac-directed expression of the human adenylyl cyclase type 8 (AC8). *FASEB J*. 2003;17:1380-1391.
25. Xiao RP, Hohl C, Altschuld R, Jones L, Livingston B, Ziman B, Tantini B, Lakatta EG. Beta 2-adrenergic receptor-stimulated increase in cAMP in rat heart cells is not coupled to changes in Ca<sup>2+</sup> dynamics, contractility, or phospholamban phosphorylation. *J Biol Chem*. 1994;269:19151-19156.
26. Laflamme MA, Becker PL. Do beta 2-adrenergic receptors modulate Ca<sup>2+</sup> in adult rat ventricular myocytes? *Am J Physiol*. 1998;274:H1308-H1314.
27. Juan-Fita MJ, Vargas ML, Hernandez J. The phosphodiesterase 3 inhibitor cilostamide enhances inotropic responses to glucagon but not to dobutamine in rat ventricular myocardium. *Eur J Pharmacol*. 2005;512:207-213.
28. Juan-Fita MJ, Vargas ML, Kaumann AJ, Hernandez Cascales J. Rolipram reduces the inotropic tachyphylaxis of glucagon in rat ventricular myocardium. *Naunyn Schmiedebergs Arch Pharmacol*. 2004;370:324-329.
29. Buxton IL, Brunton LL. Compartments of cyclic AMP and protein kinase in mammalian cardiomyocytes. *J Biol Chem*. 1983;258:10233-10239.
30. Brady JD, Rich TC, Le X, Stafford K, Fowler CJ, Lynch L, Karpen JW, Brown RL, Martens JR. Functional role of lipid raft microdomains in cyclic nucleotide-gated channel activation. *Mol Pharmacol*. 2004;65:503-511.
31. Rybin VO, Pak E, Alcott S, Steinberg SF. Developmental changes in beta2-adrenergic



- receptor signaling in ventricular myocytes: the role of Gi proteins and caveolae microdomains. *Mol Pharmacol.* 2003;63:1338-1348.
32. Head BP, Patel HH, Roth DM, Lai NC, Niesman IR, Farquhar MG, Insel PA. G-protein-coupled receptor signaling components localize in both sarcolemmal and intracellular caveolin-3-associated microdomains in adult cardiac myocytes. *J Biol Chem.* 2005;280:31036-31044.
33. Calaghan S, White E. Caveolae modulate excitation-contraction coupling and beta(2)-adrenergic signalling in adult rat ventricular myocytes. *Cardiovasc Res.* 2006;69:816-824.
34. Ostrom RS, Gregorian C, Drenan RM, Xiang Y, Regan JW, Insel PA. Receptor number and caveolar co-localization determine receptor coupling efficiency to adenylyl cyclase. *J Biol Chem.* 2001;276:42063-42069.
35. Stoclet J-C, Keravis T, Komasa N, Lugnier C. Cyclic nucleotide phosphodiesterases as therapeutic targets in cardiovascular diseases. *Expert Opin. Invest. Drugs* 1995;4:1081-1100.
36. Verde I, Vandecasteele G, Lezoualc'h F, Fischmeister R. Characterization of the cyclic nucleotide phosphodiesterase subtypes involved in the regulation of the L-type Ca<sup>2+</sup> current in rat ventricular myocytes. *Br J Pharmacol.* 1999;127:65-74.
37. Conti M, Richter W, Mehats C, Livera G, Park JY, Jin C. Cyclic AMP-specific PDE4 phosphodiesterases as critical components of cyclic AMP signaling. *J Biol Chem.* 2003;278:5493-5496.
38. Houslay MD, Adams DR. PDE4 cAMP phosphodiesterases: modular enzymes that

- orchestrate signalling cross-talk, desensitization and compartmentalization. *Biochem J.* 2003;370:1-18.
39. Richter W, Jin SL, Conti M. Splice variants of the cyclic nucleotide phosphodiesterase PDE4D are differentially expressed and regulated in rat tissue. *Biochem J.* 2005;388:803-811.
40. Bolger GB, McCahill A, Huston E, Cheung YF, McSorley T, Baillie GS, Houslay MD. The unique amino-terminal region of the PDE4D5 cAMP phosphodiesterase isoform confers preferential interaction with beta-arrestins. *J Biol Chem.* 2003;278:49230-49238.
41. Méry PF, Lohmann SM, Walter U, Fischmeister R. Ca<sup>2+</sup> current is regulated by cyclic GMP-dependent protein kinase in mammalian cardiac myocytes. *Proc Natl Acad Sci U S A.* 1991;88:1197-1201.
42. Vandecasteele G, Verde I, Rucker-Martin C, Donzeau-Gouge P, Fischmeister R. Cyclic GMP regulation of the L-type Ca(2+) channel current in human atrial myocytes. *J Physiol.* 2001;533:329-340.
43. Movsesian MA, Smith CJ, Krall J, Bristow MR, Manganiello VC. Sarcoplasmic reticulum-associated cyclic adenosine 5'-monophosphate phosphodiesterase activity in normal and failing human hearts. *J Clin Invest.* 1991;88:15-19.
44. Méry PF, Brechler V, Pavoine C, Pecker F, Fischmeister R. Glucagon stimulates the cardiac Ca<sup>2+</sup> current by activation of adenylyl cyclase and inhibition of phosphodiesterase. *Nature.* 1990;345:158-161.
45. Lohse MJ, Engelhardt S, Eschenhagen T. What is the role of beta-adrenergic signaling

in heart failure? *Circ Res.* 2003;93:896-906.

46. Smith CJ, Huang R, Sun D, Ricketts S, Hoegler C, Ding JZ, Moggio RA, Hintze TH. Development of decompensated dilated cardiomyopathy is associated with decreased gene expression and activity of the milrinone-sensitive cAMP phosphodiesterase PDE3A. *Circulation* 1997;96:3116-3123.
47. Sato N, Asai K, Okumura S, Takagi G, Shannon RP, Fujita-Yamaguchi Y, Ishikawa Y, Vatner SF, Vatner DE. Mechanisms of desensitization to a PDE inhibitor (milrinone) in conscious dogs with heart failure. *Am J Physiol.* 1999;276:H1699-H1705.
48. Ding B, Abe J, Wei H, Huang Q, Walsh RA, Molina CA, Zhao A, Sadoshima J, Blaxall BC, Berk BC, Yan C. Functional role of phosphodiesterase 3 in cardiomyocyte apoptosis: implication in heart failure. *Circulation.* 2005;111:2469-2476.
49. Takahashi K, Osanai T, Nakano T, Wakui M, Okumura K. Enhanced activities and gene expression of phosphodiesterase types 3 and 4 in pressure-induced congestive heart failure. *Heart Vessels* 2002;16:249-256.
50. Lehnart SE, Wehrens XH, Reiken S, Warrier S, Belevych AE, Harvey RD, Richter W, Jin SL, Conti M, Marks AR. Phosphodiesterase 4D deficiency in the ryanodine-receptor complex promotes heart failure and arrhythmias. *Cell* 2005;123:25-35.

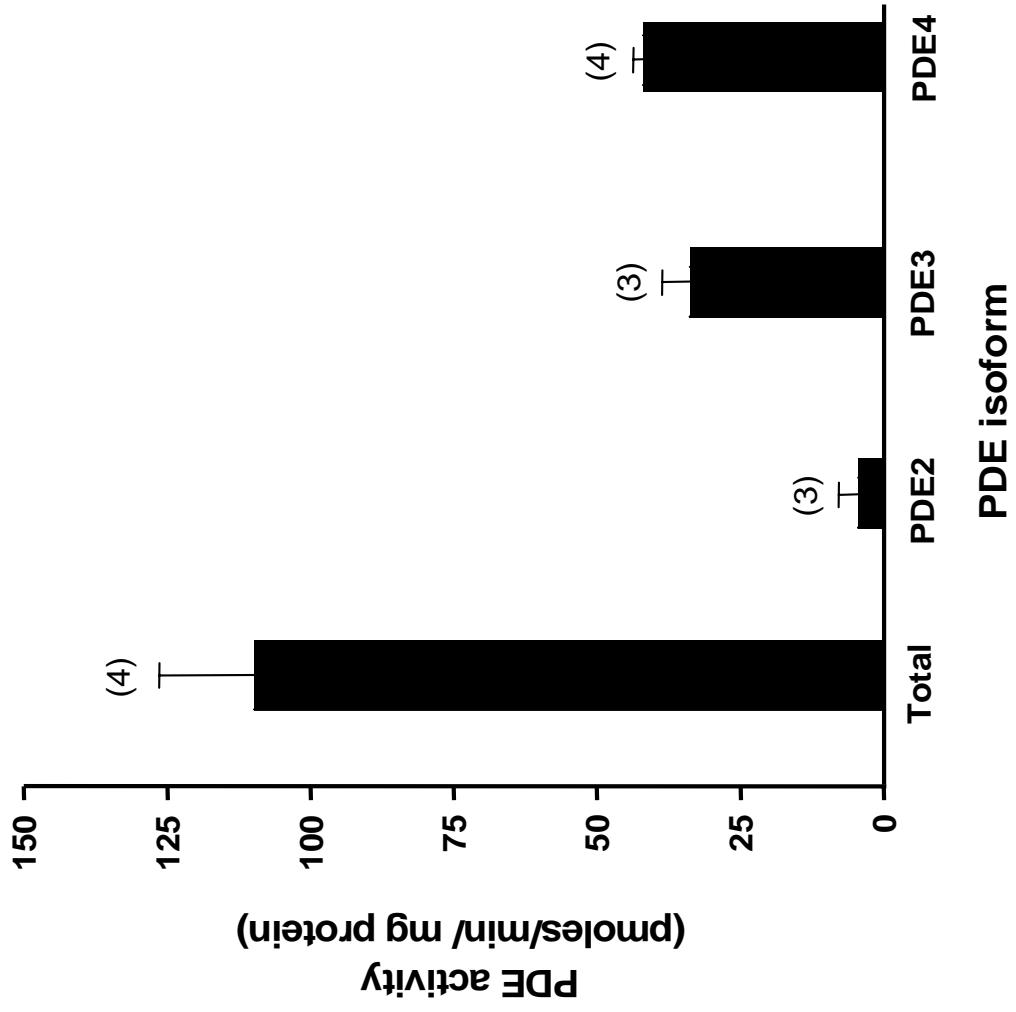


Figure 1

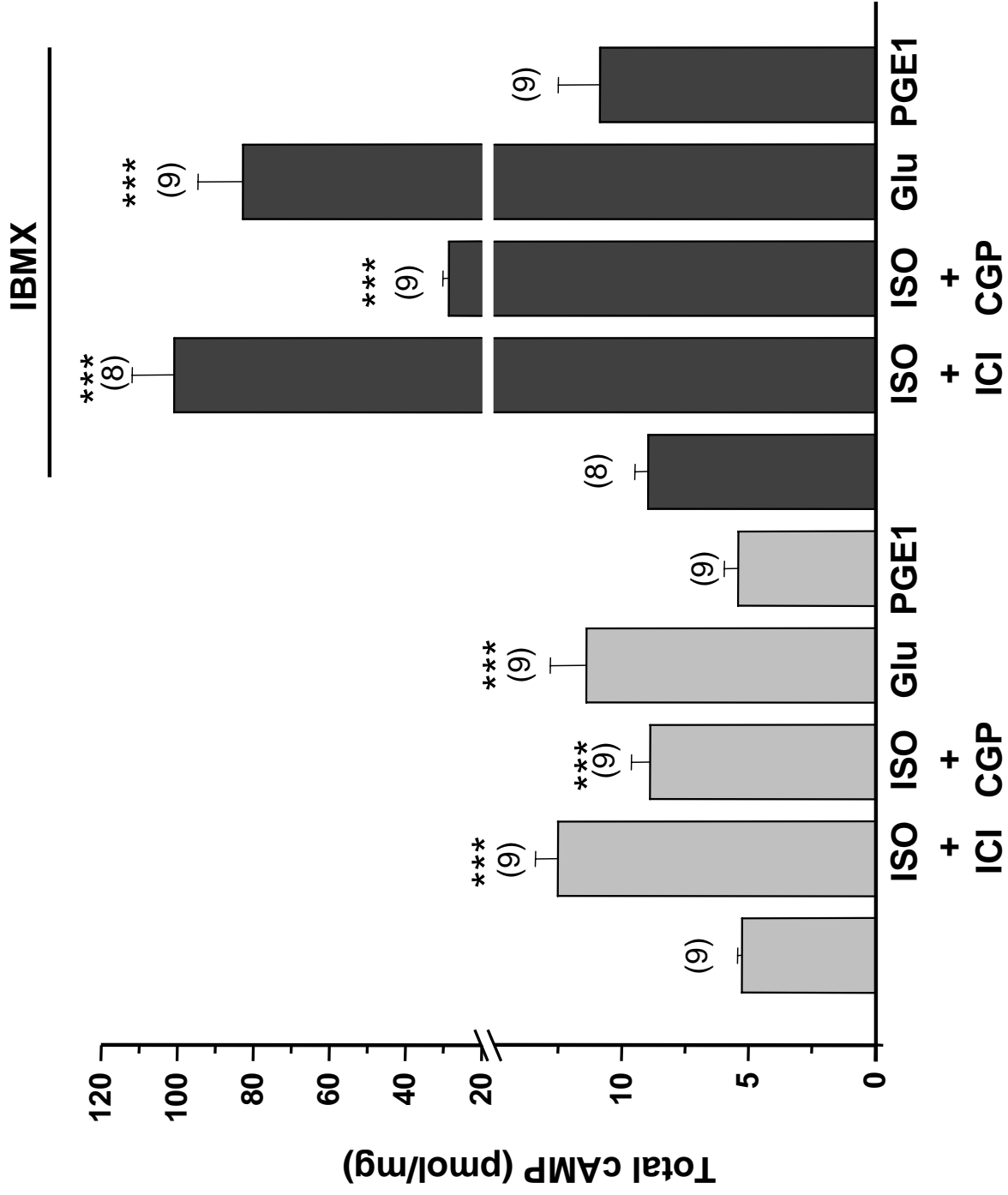


Figure 2

CIRCRESAHA/2006/124800/R1

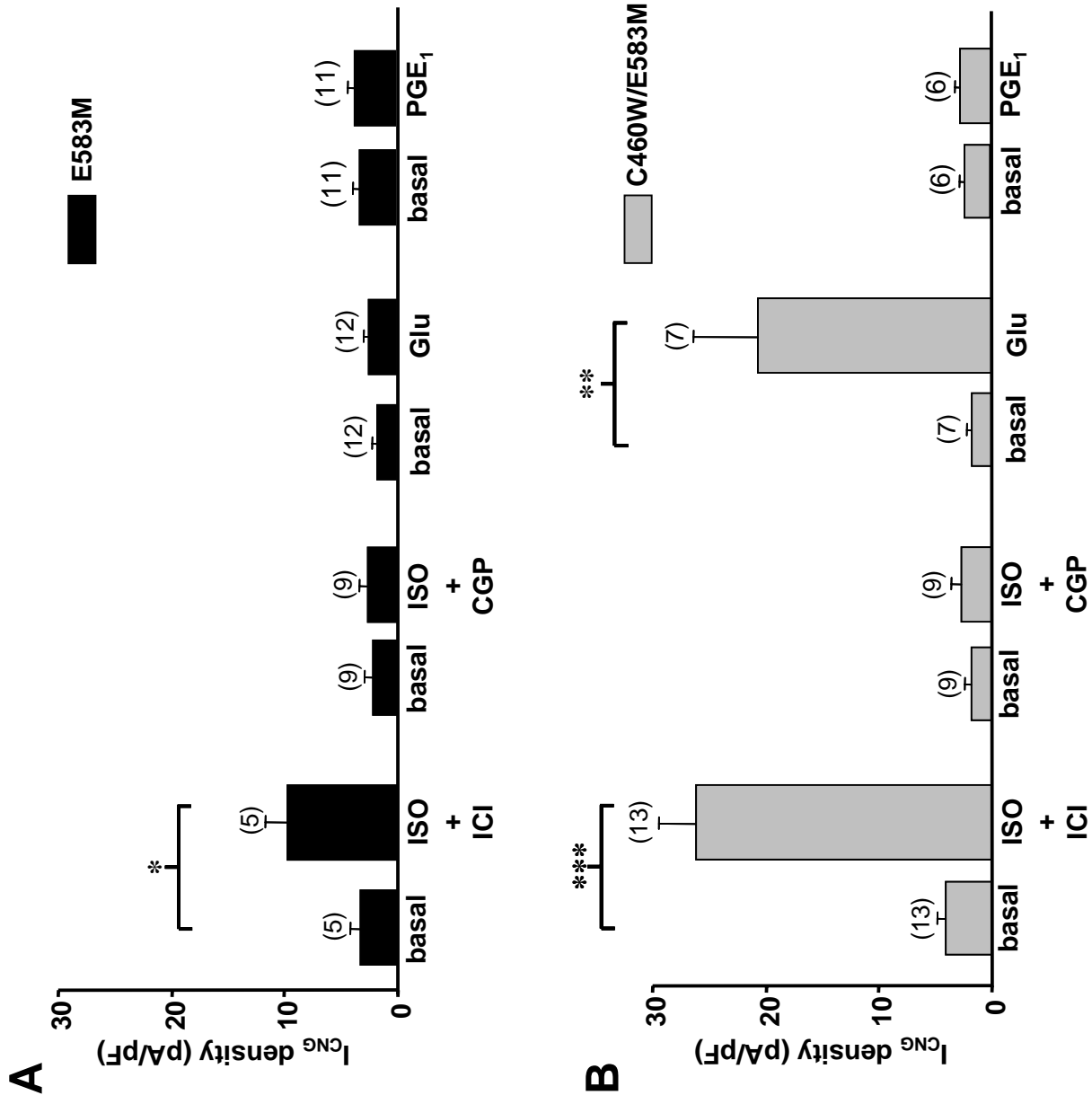


Figure 3

CIRCRESAHA/2006/124800/R1

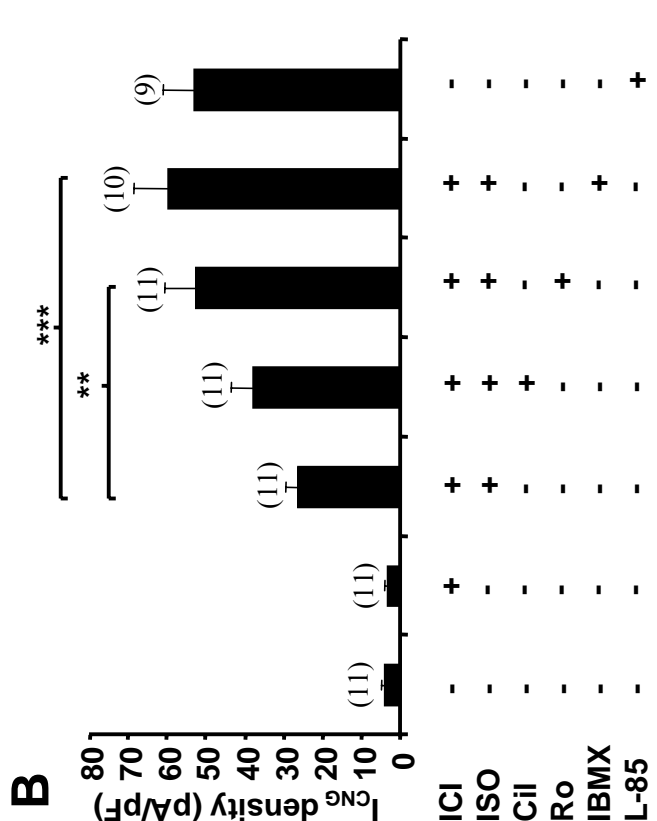
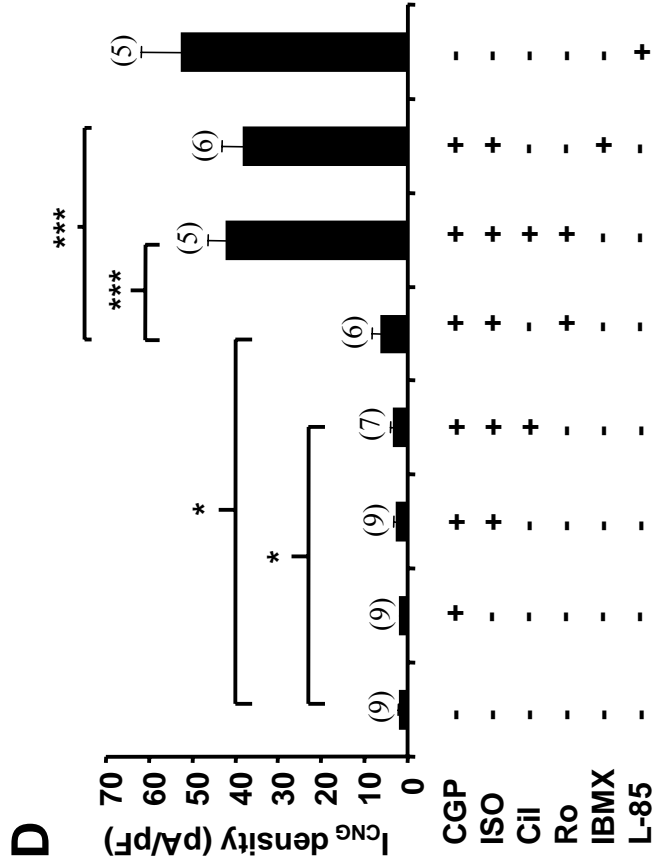
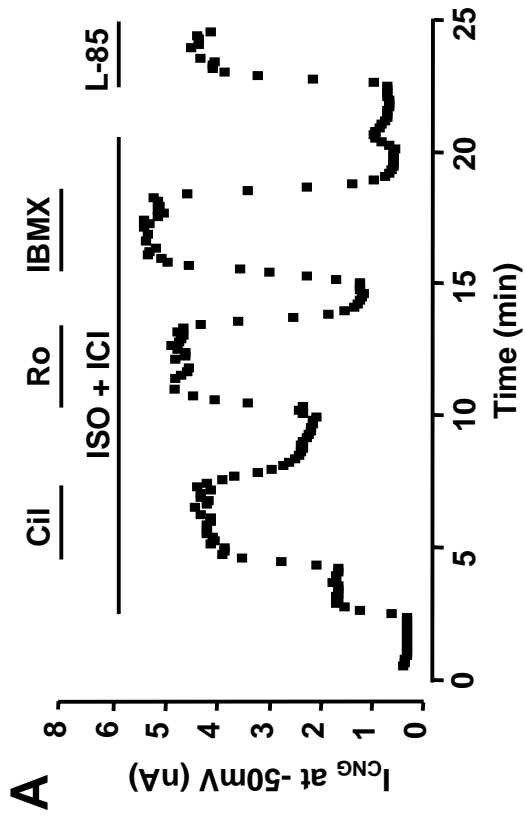
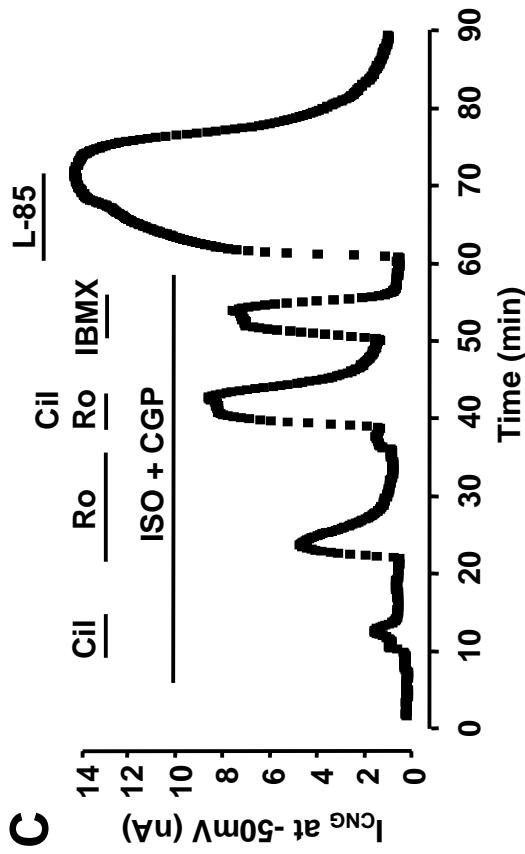


Figure 4

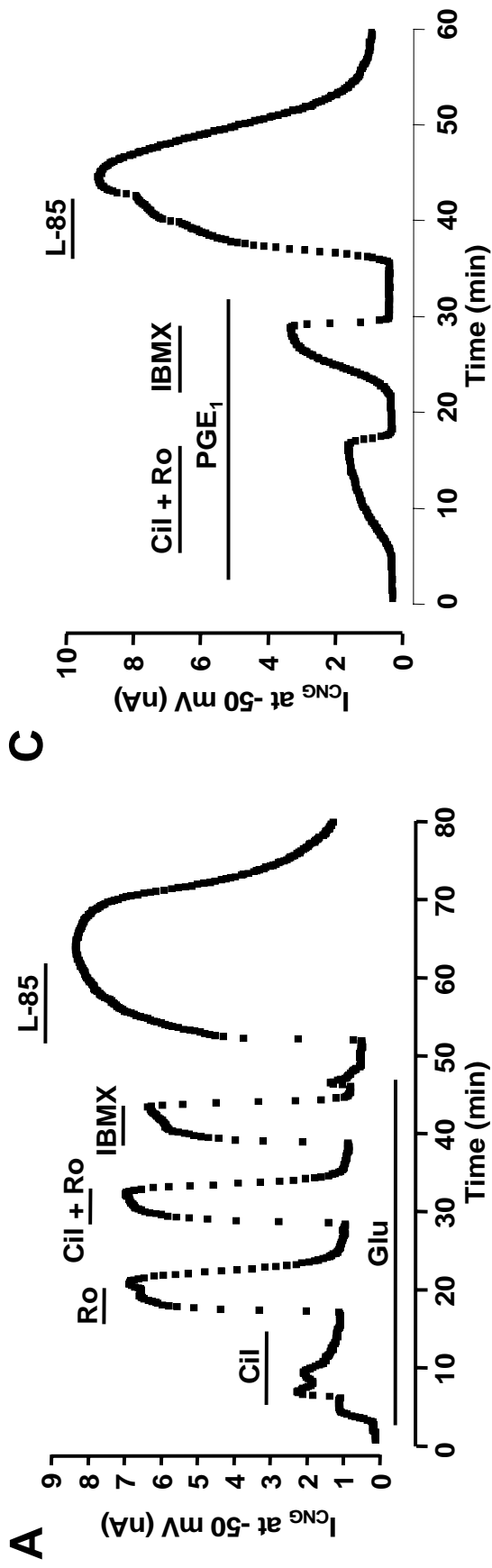


Figure 5



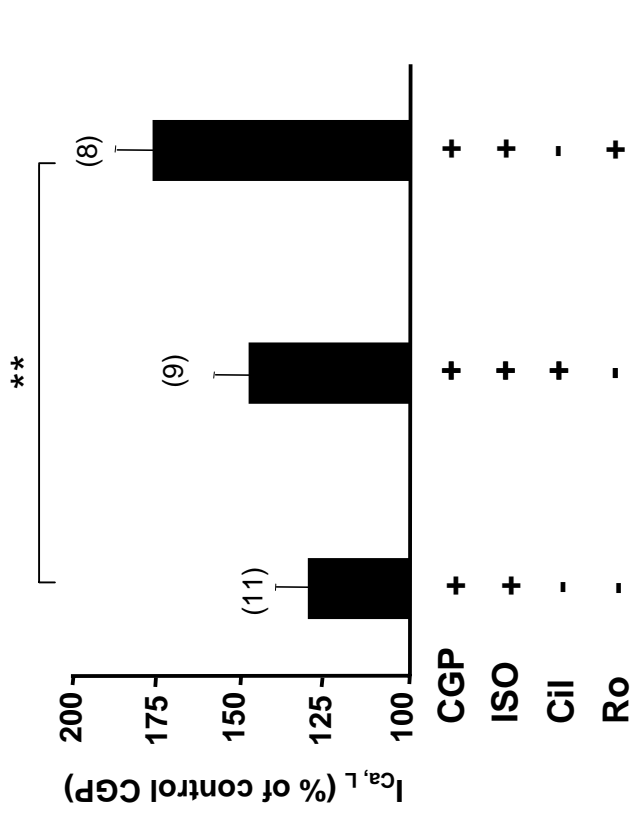
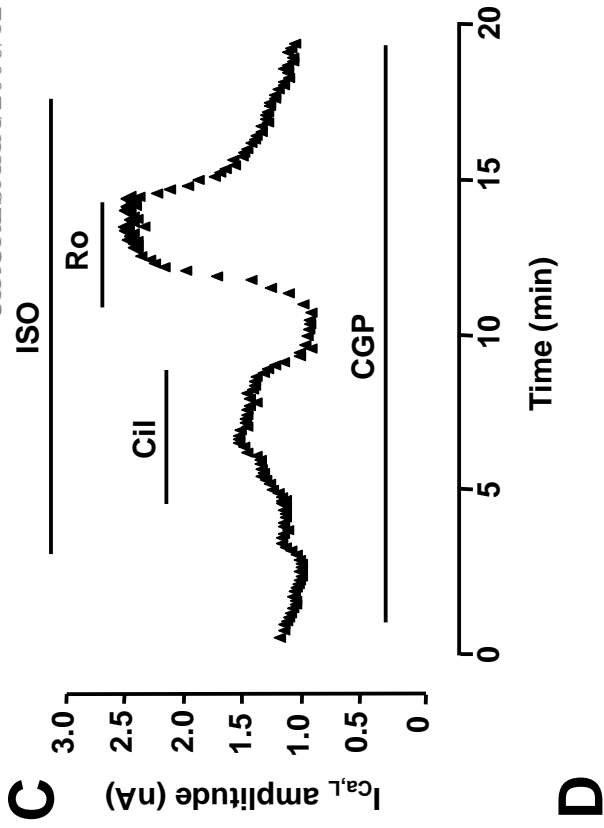
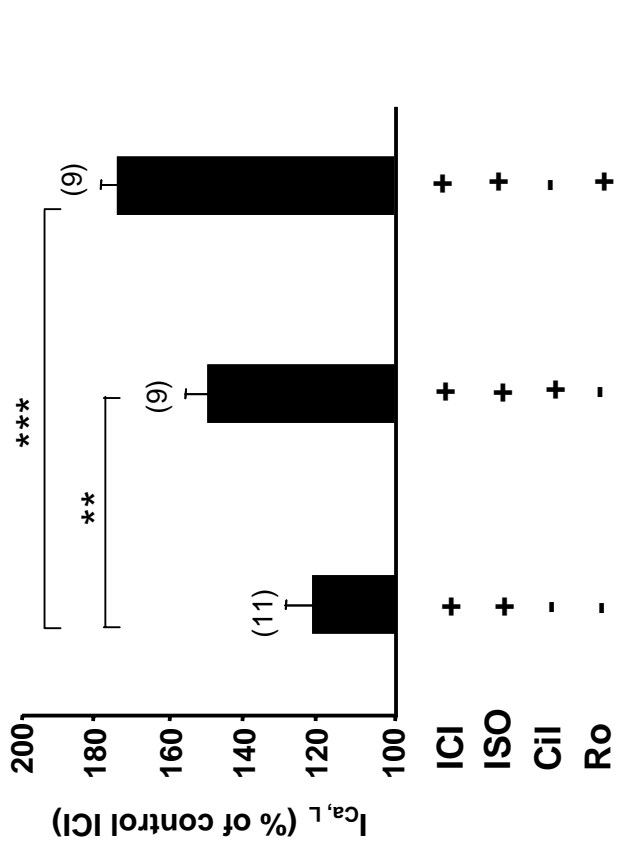
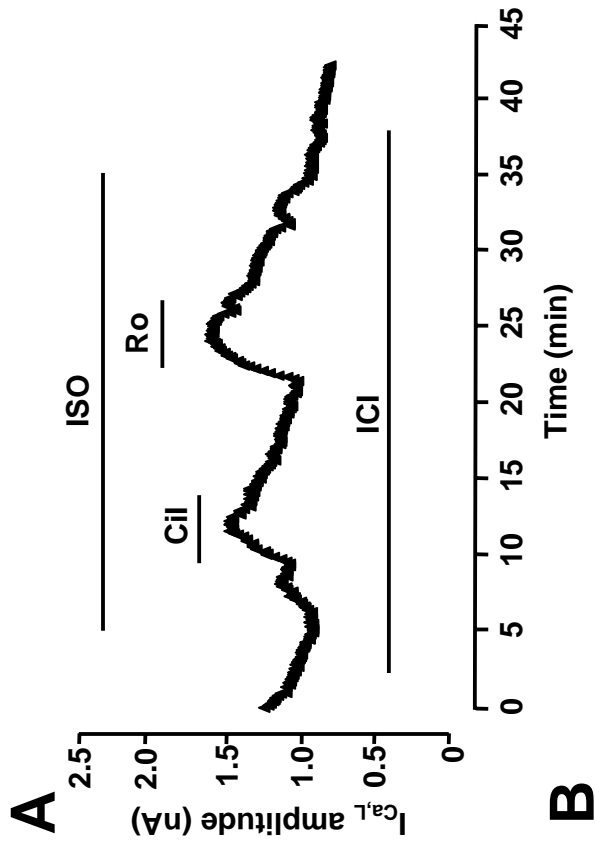


Figure 6

CIRCRESAHA/2006/124800/R1

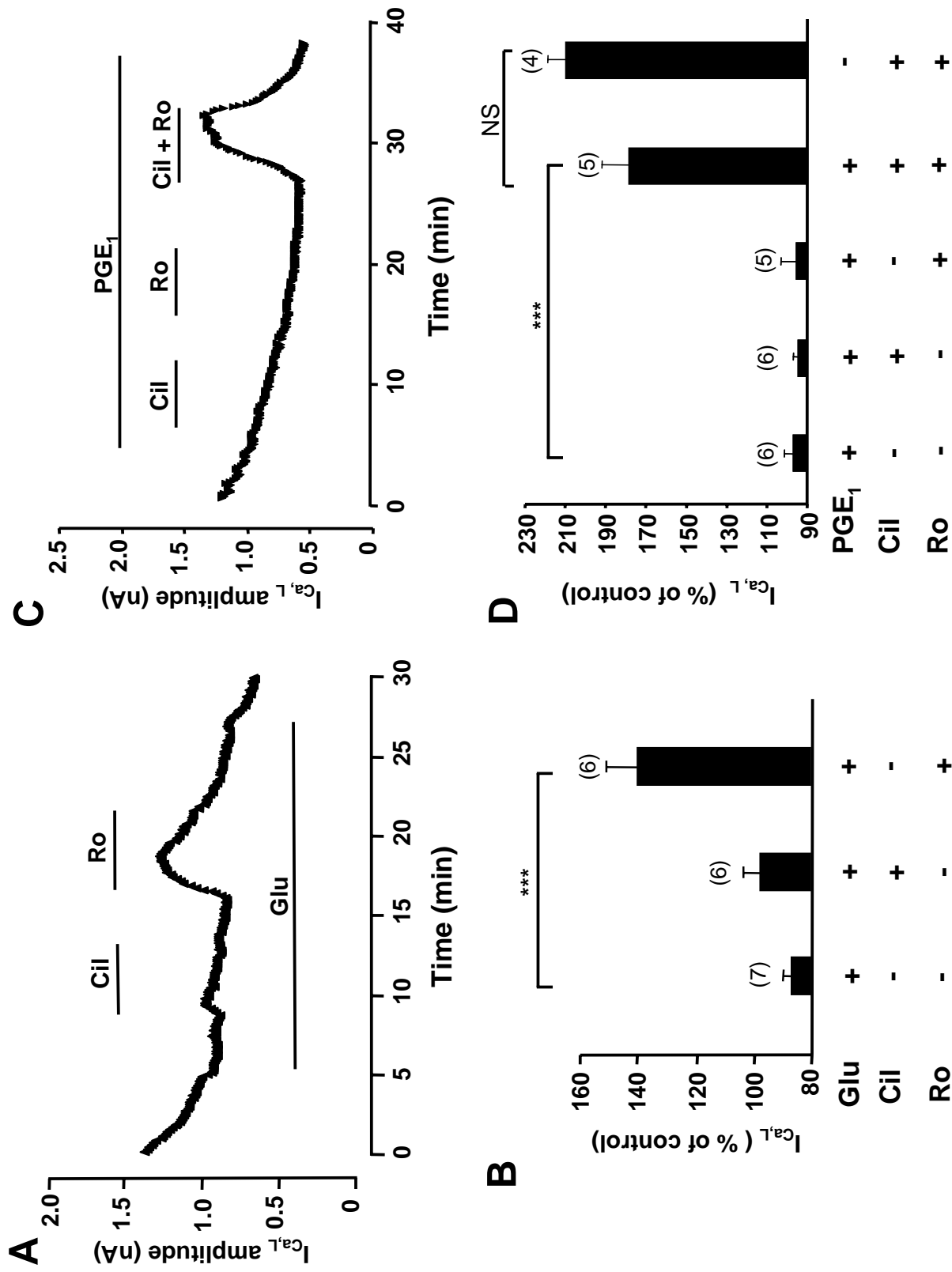


Figure 7

**DATA SUPPLEMENT TO MANUSCRIPT CIRCRESAHA/2006/124800****Material and Methods**

*Isolation, Culture and Infection of ARVM* - The investigation conforms with the European Community guiding principles in the care and use of animals (86/609/CEE, *CE Off J* n°L358, 18 December 1986), the local ethics committee (CREEA Ile-de-France Sud) guidelines and the French decree n°87/748 of October 19, 1987 (*J Off République Française*, 20 October 1987, pp. 12245-12248). Authorizations to perform animal experiments according to this decree were obtained from the French Ministère de l'Agriculture et de la Forêt (n°7475, May 27, 1997). Male Wistar rats (160-180 g) were subjected to anesthesia by intraperitoneal injection of pentothal (0.1 mg/g) and hearts were excised rapidly. Individual ARVMs were obtained by retrograde perfusion of the heart as previously described.<sup>1</sup> Freshly isolated cells were suspended in minimal essential medium (MEM: M 4780; Sigma, St. Louis, USA) containing 1.2 mmol/L  $\text{Ca}^{2+}$ , 2.5% fetal bovine serum (FBS, Invitrogen, Cergy-Pontoise, France), 1% penicillin-streptomycin and 2% HEPES (pH 7.6) and plated on laminin coated culture dishes (10  $\mu\text{g/mL}$  laminin, 2h) at a density of  $10^4$  cells per dish. The cells were left to adhere for 1 hour in a 95%  $\text{O}_2$ , 5%  $\text{CO}_2$  incubator at 37°C, before the medium was replaced by 400  $\mu\text{L}$  of FBS-free MEM. For experiments with CNG channels, the E583M or the C460W/E583M CNGA2-encoding adenovirus were added to 200  $\mu\text{L}$  of MEM at a multiplicity of infection (MOI) of 3000 pfu/cell. After 2 hours, the same volume of FBS-free medium without adenovirus was added and the cells were placed overnight in incubator. The medium was changed the next morning for adenovirus- and FBS-free MEM. Patch-clamp experiments were performed the same day.

*Electrophysiological Experiments* - The whole-cell configuration of the patch-clamp technique was used to record the L-type calcium current ( $I_{\text{Ca,L}}$ ) and the CNG current ( $I_{\text{CNG}}$ ), as previously described.<sup>2</sup> For  $I_{\text{Ca,L}}$  measurement, the cells were depolarized every 8 seconds to 0

mV during 400 ms. Fast sodium current was inactivated by holding potential (-50 mV) and potassium currents were blocked by replacing all  $K^+$  ions with external and internal  $Cs^+$ . For  $I_{CNG}$  measurement, the cells were maintained at 0 mV holding potential and routinely hyperpolarized every 8 seconds to -50 mV test potential during 200 ms. The 0 mV holding potential was chosen because it corresponds to the reversal potential of  $I_{CNG}$  under our experimental conditions.  $I_{CNG}$  was recorded in the absence of divalent cations in the extracellular solution allowing monovalent cations to flow through the channels in an unspecific manner. All the experiments were done at room temperature (21-27°C), and the temperature did not vary by more than 1°C in a given experiment.

*Solutions and Drugs for Patch-clamp Recording* - Control zero- $Ca^{2+}/Mg^{2+}$  extracellular  $Cs^+$  Ringer solution contained (in mmol/L): NaCl 107.1, CsCl 20,  $NaHCO_3$  4,  $NaH_2PO_4$  0.8, D-Glucose 5, sodium pyruvate 5, HEPES 10, adjusted to pH 7.4 with NaOH. For  $I_{CNG}$  recording, this solution was supplemented with nifedipine (1  $\mu$ mole/L) to block nonspecific cation current through L-type  $Ca^{2+}$  channels. For  $I_{Ca,L}$  recording, nifedipine was omitted and 1.8 mM  $CaCl_2$  and 1.8 mM  $MgCl_2$  were added to the external solution. Control and drug-containing solutions were applied to the exterior of the cell by placing the cell at the opening of a 250  $\mu$ m inner diameter capillary tubing. Patch electrodes (0.8-1.2 M $\Omega$ ) were filled with control internal solution containing (in mmol/L): CsCl 118, EGTA 5,  $MgCl_2$  4, sodium phosphocreatine 5,  $Na_2ATP$  3.1,  $Na_2GTP$  0.42,  $CaCl_2$  0.062 (pCa 8.5), HEPES 10, adjusted to pH 7.3 with CsOH. Isoprenaline (ISO), prostaglandin  $E_1$  ( $PGE_1$ ), glucagon, ICI 118551 (ICI), CGP 20712A (CGP), rolipram, erythro-9-(2-hydroxy-3-nonyl)adenine (EHNA) and 3-isobutyl-1-methyl-xanthine (IBMX) were purchased from Sigma. L-858051 (L-85, a hydrosoluble analogue of forskolin) and cilostamide were purchased from France Biochem (Meudon, France). Ro 20-1724 (Ro) was kindly provided by Hoffman-La-Roche (Basel,

Switzerland), piclamilast by Sanofi-Aventis (Paris, France) and RS25344 by Roche (Palo Alto, CA, USA).

*PDE Assay* - Freshly isolated ARVMs were seeded on 35 mm Petri dishes at a density of  $10^5$  cells/dish in FBS-free medium. After 1h, cells were washed with PBS and homogenized in ice-cold buffer containing (in mmol/L) NaCl 150, sodium phosphate buffer (pH 7.2) 10, EDTA 2,  $\beta$ -mercaptoethanol 5, sodium pyrophosphate 30, sodium fluoride 50, benzamidine 3, AEBSF 2, NP40 0.1%, leupeptin 5  $\mu\text{g/ml}$ , pepstatin 20  $\mu\text{g/ml}$ , microcystin 1  $\mu\text{M}$ . PDE activity was measured according to a modification of the two-step assay procedure method described by Thompson & Appleman<sup>3</sup> in a total volume of 200  $\mu\text{L}$  including (in mmol/L) Tris-HCl 40, pH 8.0,  $\text{MgCl}_2$  10,  $\beta$ -mercaptoethanol 1.25 supplemented with 1  $\mu\text{M}$  cAMP and  $10^5$  cpm [ $^3\text{H}$ ]-cAMP, as detailed previously.<sup>4</sup> PDE family-specific activities were determined as the difference between PDE activity in the absence of inhibitor and the residual hydrolytic activity observed in the presence of the selective inhibitor. Protein concentration was determined by bicinchonic acid assay after addition of deoxycholate and precipitation by trichloroacetic acid (0.1%).

*cAMP Level Determination* - Freshly isolated ARVMs suspended in FBS-free MEM were plated in laminin-coated 12-well plates at a density of  $5 \times 10^4$  cells/well. After 1h, the medium was replaced with control zero  $\text{Ca}^{2+}/\text{Mg}^{2+}$  extracellular  $\text{Cs}^+$  Ringer solution in the presence or absence of  $\beta$ -adrenergic antagonists ICI (1 $\mu\text{mol/L}$ ) or CGP (1  $\mu\text{mol/L}$ ), or IBMX (100  $\mu\text{mol/L}$ ). After 15 min., the same Ringer solution with or without receptor agonists (ISO, 1  $\mu\text{mol/L}$ ; glucagon, 1  $\mu\text{mol/L}$ ; or  $\text{PGE}_1$ , 1  $\mu\text{mol/L}$ ) was applied for 3 min at room temperature. The stimulation was stopped by ice-cold trichloroacetic acid (0.1%) in 95% EtOH. After 30 min incubation on ice, samples were scraped and centrifuged for 30 min at 3,000 rpm at 4°C. The pellet was dissolved in 5% SDS in 0.1 N NaOH for protein determination by bicinchonic acid assay. EtOH in the supernatant was evaporated and the material was

reconstituted with PBS, pH 7.4, then cAMP was measured by RIA after acetylation of the samples and appropriate dilution.<sup>5,6</sup>

## Results

For each receptor, identical experiments were performed in myocytes expressing the low affinity cAMP sensor E583M CNGA2, and gave essentially similar results. As shown in supplementary Fig IA and IB, individual inhibition of PDE3 and PDE4 potentiated the  $\beta_1$ -AR response, and these effects were not different from the effect of IBMX. In contrast, simultaneous inhibition of PDE3 and PDE4 was necessary to unmask a substantial and sustained sarcolemmal cAMP accumulation in response to  $\beta_2$ -AR stimulation (supplementary Fig IC and ID), showing that either PDE3 or PDE4 activity is enough to dampen  $\beta_2$ -AR cAMP at the membrane. As noted above,  $I_{\text{CNG}}$  was not augmented by cell stimulation with glucagon when using the low affinity CNG channel (Fig. IIA and IIB). However, similarly to what observed with the C460W/E583M mutant, selective blockade of PDE3 failed to increase  $I_{\text{CNG}}$  while PDE4 inhibition induced a major rise in  $I_{\text{CNG}}$ . Supplementary Fig. IIC and IID present the results obtained when PGE<sub>1</sub> was used to trigger cAMP in cardiac myocytes. While the hormone alone failed to increase  $I_{\text{CNG}}$ , the additional and concomitant inhibition of PDE3 and PDE4 provoked a slow accumulation of cAMP at the membrane. This accumulation was enhanced when all PDEs were inhibited with IBMX (supplementary Fig. IIC and IID).

## Legends to Supplementary Figures

**Supplementary Figure I.** PDE regulation of cAMP signals from  $\beta_1$ -AR and  $\beta_2$ -AR. A and C, Time course of  $I_{\text{CNG}}$  in adult rat ventricular myocytes expressing E583M CNGA2. The cells were superfused for a few minutes with a control solution and then challenged with a drug

during the periods indicated with the solid lines. B and D, Summary of the results obtained in a series of experiments as in A and C, respectively. Specific activation of  $\beta_1$ -AR and  $\beta_2$ -AR as in Fig. 1. Cilostamide (Cil, 1  $\mu\text{mol/L}$ ) was used for specific inhibition of PDE3 and Ro 20-1724 (Ro, 10  $\mu\text{mol/L}$ ) for specific inhibition of PDE4. IBMX (100  $\mu\text{mol/L}$ ) was used for non specific inhibition of PDEs. At the end of the experiment, the cell was challenged with a saturating concentration of the forskolin analog L-858051 (L-85, 100  $\mu\text{mol/L}$ ) as an internal control for CNG channels expression. The bars show the means $\pm$ s.e.m. of the number of cells indicated. Statistically significant differences are indicated as \*\*,  $p<0.01$  and \*\*\*,  $p<0.001$ .

**Supplementary Figure II.** PDE regulation of cAMP signals from Glu-R and PGE<sub>1</sub>-R. A and C, Adult rat ventricular myocytes infected with E583M Ad-CNG for 24h were superfused for a few minutes with a control Ringer solution and then challenged with a drug during the periods indicated with the solid lines. B and D, Summary of the results obtained in a series of experiments as in A and C, respectively. Glu-R activation was achieved by application of glucagon (Glu, 1  $\mu\text{mol/L}$ ). Pharmacological inhibition of PDEs as in Fig.2. Experiment was terminated with application of 100  $\mu\text{mol/L}$  L-85. The bars show the means $\pm$ s.e.m. of the number of cells indicated. Statistically significant differences are indicated as \*,  $p<0.05$ ; \*\*,  $p<0.01$  and \*\*\*,  $p<0.001$ . NS, non significant.

### Supplementary references

- 1-Verde I, Vandecasteele G, Lezoualc'h F, Fischmeister R. Characterization of the cyclic nucleotide phosphodiesterase subtypes involved in the regulation of the L-type Ca<sup>2+</sup> current in rat ventricular myocytes. *Br J Pharmacol.* 1999;127:65-74.
- 2-Rochais F, Vandecasteele G, Lefebvre F, Lugnier C, Lum H, Mazet JL, Cooper DM,

Fischmeister R. Negative feedback exerted by cAMP-dependent protein kinase and cAMP phosphodiesterase on subsarcolemmal cAMP signals in intact cardiac myocytes: an in vivo study using adenovirus-mediated expression of CNG channels. *J Biol Chem.* 2004;279:52095-105.

3-Thompson WJ, Appleman MM. Multiple cyclic nucleotide phosphodiesterase activities from rat brain. *Biochemistry.* 1971;10:311-6.

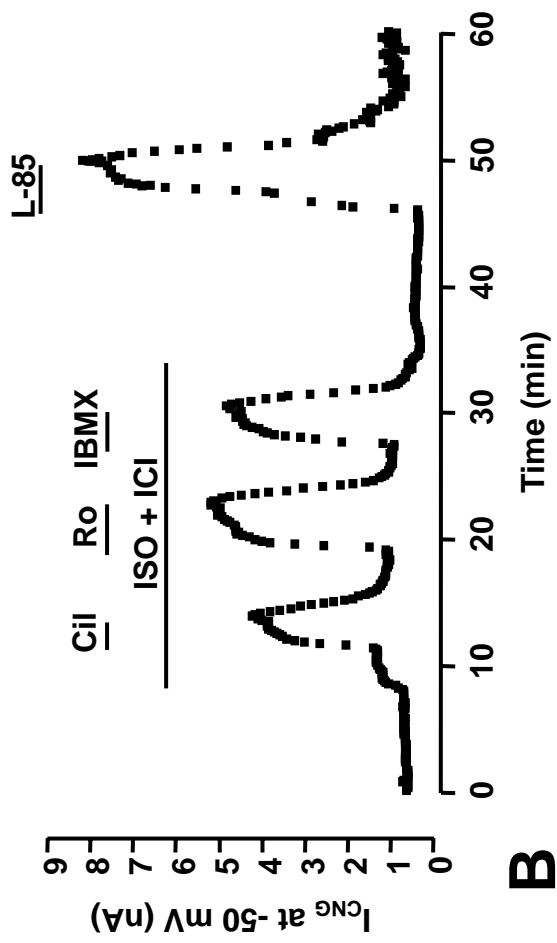
4-Oki N, Takahashi SI, Hidaka H, Conti M. Short term feedback regulation of cAMP in FRTL-5 thyroid cells. Role of PDE4D3 phosphodiesterase activation. *J Biol Chem.* 2000;275:10831-7.

5-Harper JF, Brooker G. Femtomole sensitive radioimmunoassay for cyclic AMP and cyclic GMP after 2'0 acetylation by acetic anhydride in aqueous solution. *J Cyclic Nucleotide Res.* 1975;1:207-18.

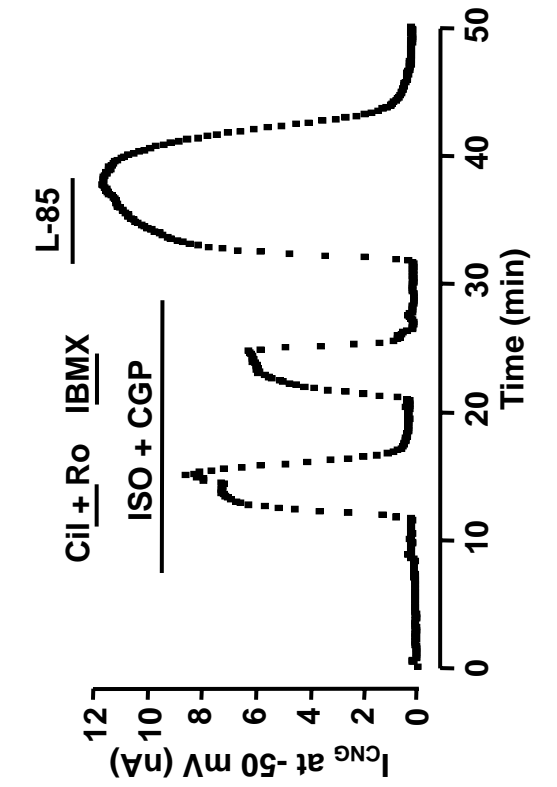
6-Steiner AL, Pagliara AS, Chase LR, Kipnis DM. Radioimmunoassay for cyclic nucleotides. II. Adenosine 3',5'-monophosphate and guanosine 3',5'-monophosphate in mammalian tissues and body fluids. *J Biol Chem.* 1972;247:1114-20.



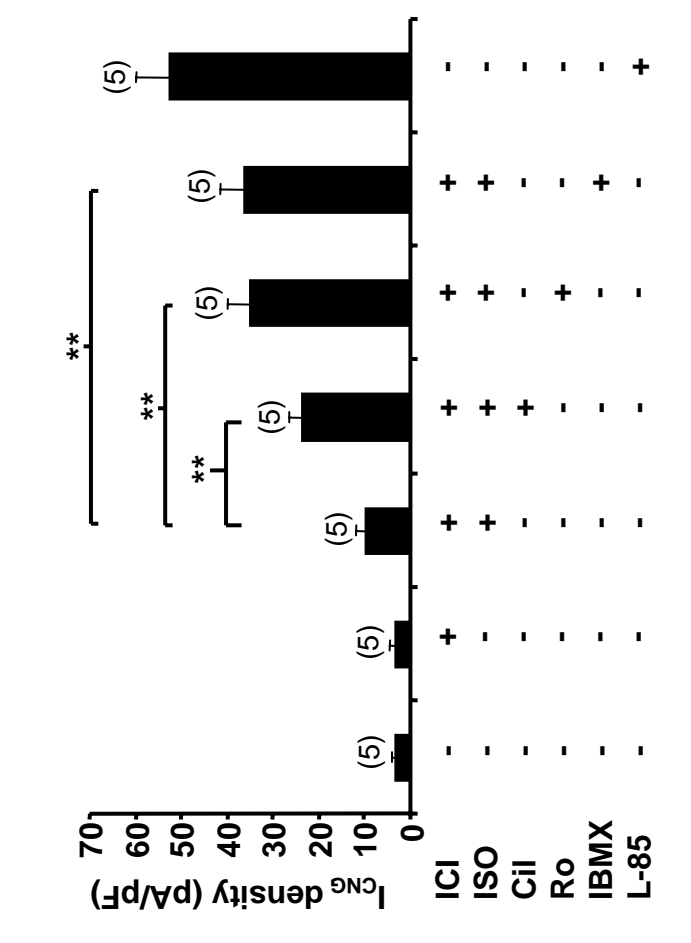
**A**



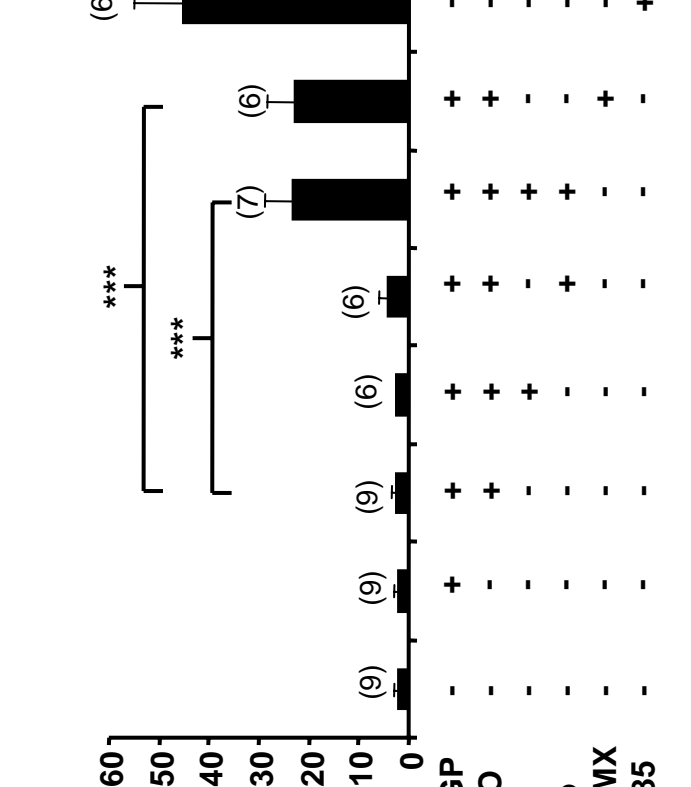
**C**

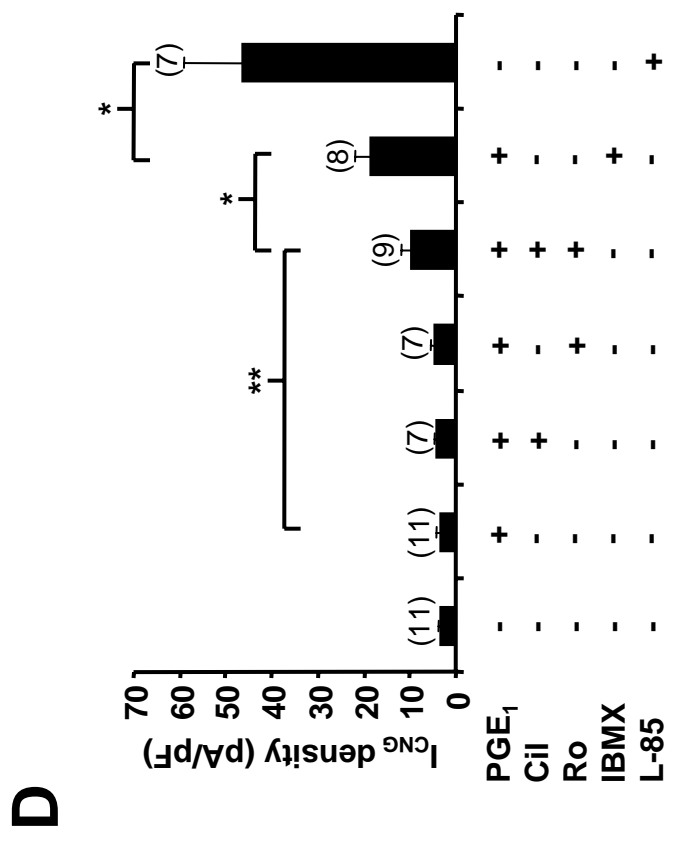
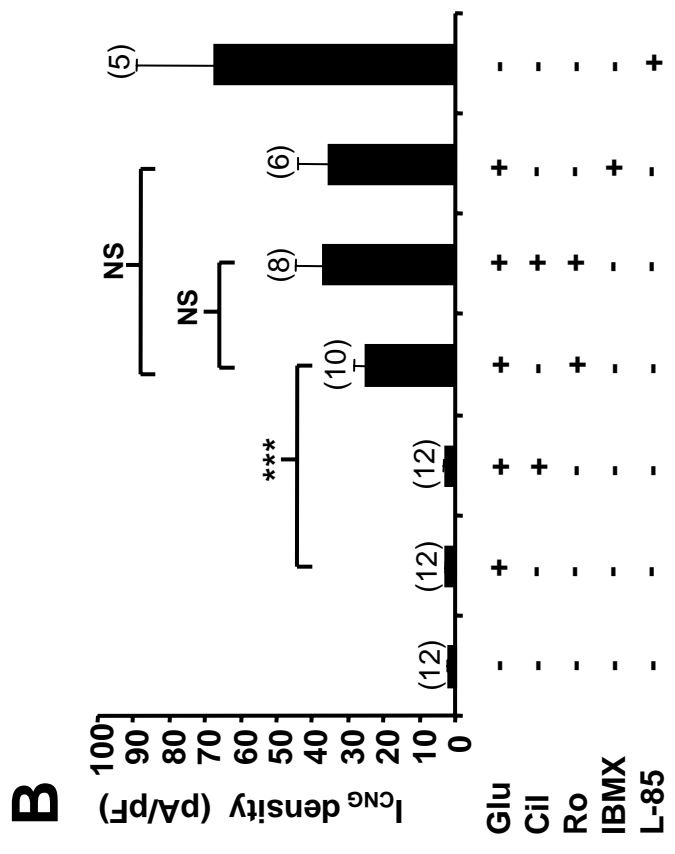
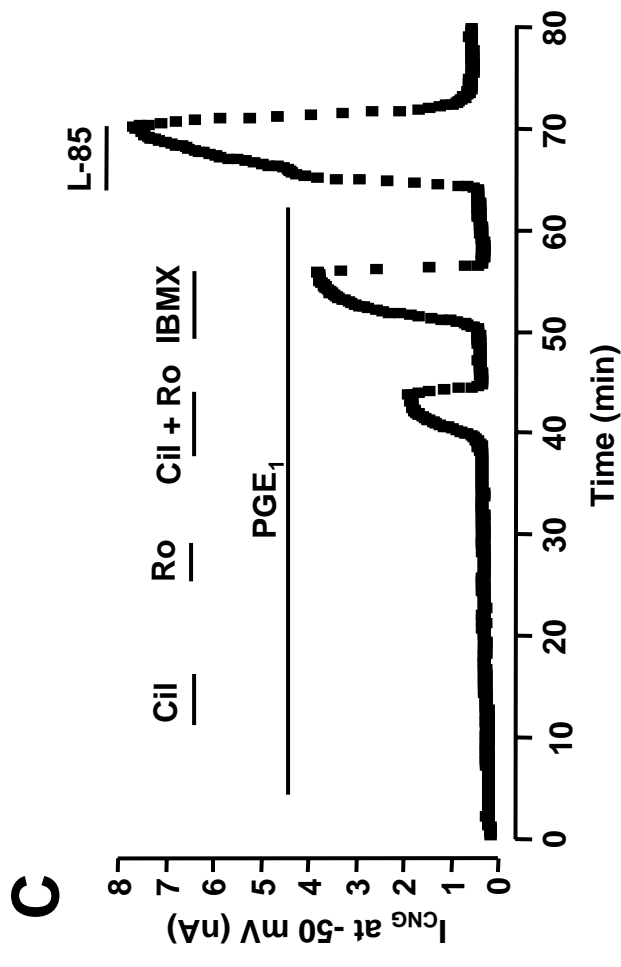
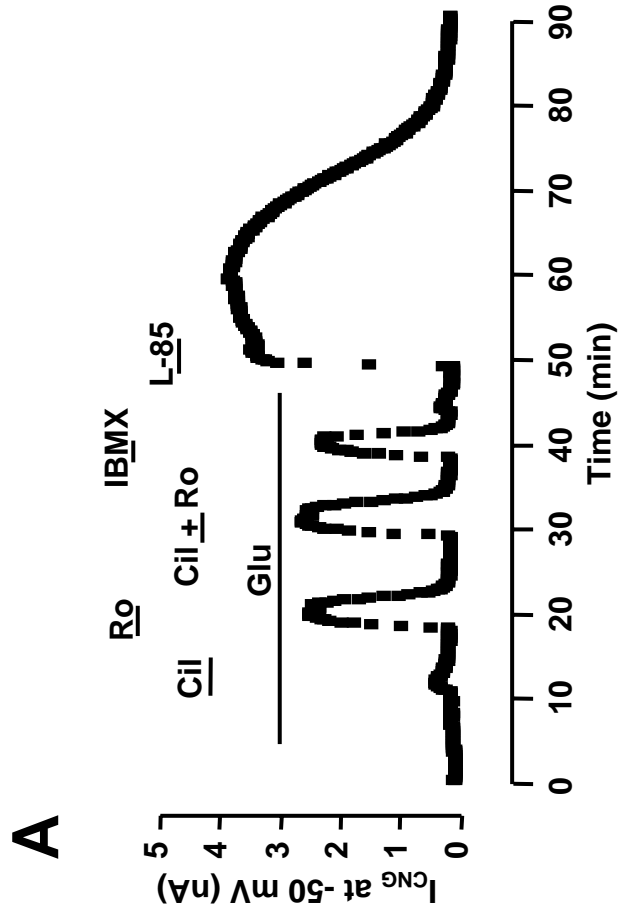


**B**



**D**





Suppl Figure II